Biogeotechnics 4 (2026) 100158

Contents lists available at ScienceDirect

Biogeotechnics

journal homepage: www.keaipublishing.com/en/journals/biogeotechnics/

Review Article

Eco-geotechnics under climate change: A state-of-the-art review

Charles Wang Wai Ng[a], Qi Zhang[a], Haowen Guo[b], Junjun Ni[c,*], Yuchen Wang[a], Anthony Kwan Leung[a], Chao Zhou[d]

[a] Department of Civil and Environmental Engineering, Hong Kong University of Science and Technology, Hong Kong SAR, China
[b] Guangzhou Institute of Energy Conversion, Chinese Academy of Sciences (CAS), Guangzhou 510640, China
[c] School of Transportation, Southeast University, Nanjing 211189, China
[d] Department of Civil and Environmental Engineering, The Hong Kong Polytechnic University, Hong Kong SAR, China

ARTICLE INFO

Keywords:
Eco-geotechnics
Vegetation
Unsaturated soil
Climate change

ABSTRACT

Global climate change has exacerbated extreme weather events, such as intense rainfall and heat waves, resulting in the deterioration of geotechnical earthen structures. To address the urgent need for sustainable development, eco-friendly solutions are being explored, with vegetation emerging as a vital natural engineer. Despite the potential of vegetation, traditional practices often limit its role to aesthetics, overlooking the engineering benefits of plant roots. This paper introduces the new interdisciplinary field of eco-geotechnics, which integrates soil mechanics, ecology, botany, and atmospheric sciences, etc. to enhance geotechnical infrastructure. By focusing on atmosphere–plant–soil interactions, this review highlights how plants contribute to the stability of earthen infrastructure through root reinforcement and hydrological benefits. This paper also reviews recent advancements in constitutive modelling of vegetated soils, particularly focusing on a novel eco-unsaturated soil model. It discusses experimental testing of vegetated soils and their wide applications. Critical research gaps are identified in terms of the effects of extreme weather on root systems, soil cracking dynamics, ecological restoration in contaminated areas, and the synergistic effects of vegetation with sustainable soil stabilisers. Additionally, the use of smart monitoring techniques based on a combination of remote sensing and machine learning is proposed to assess vegetation–soil interactions in real-time. By integrating ecological and geotechnical processes, a comprehensive framework is recommended for future research directions in eco-geotechnics, which will ultimately facilitate the development of resilient engineering solutions that can withstand the challenges posed by climate change. The insights gained will be invaluable for improving the sustainability of geotechnical practices and enhancing the resilience of infrastructures in a changing climate.

1. Introduction

In recent years, global climate change has caused an increase in the frequency of extreme weather events, such as intense rainfall and heat waves. Such extreme events lead to the gradual deterioration of geotechnical earthen structures, exemplified by shallow slope failure and soil erosion (Xu et al., 2023; Li et al., 2024). In response to the growing demand for sustainable development, engineers are exploring greener solutions to mitigate the impacts of climate change on geotechnical infrastructures. Vegetation, functioning as a natural engineer, has emerged as an alternative that provides environment-friendly solutions for bioengineered slopes, ecological restoration at mining sites, soil erosion, and windstorm mitigation. However, conventional practice often limits the role of vegetation to aesthetic purposes, neglecting the engineering functions of plant roots in geotechnical design. To bridge the gap between the current requirements and practices, an in-depth study of the atmosphere–plant–soil interaction and its influence in the geotechnical field is necessary from both theoretical and experimental perspectives (Ni et al., 2018a). Against this backdrop, a new interdisciplinary subject known as 'eco-geotechnics' has emerged recently. Eco-geotechnics integrates knowledge from soil and rock mechanics, ecology, botany, and atmosphere science. It links conventional geotechnics with the life sciences, including plants, animals, and bacteria. Researchers are leveraging the insights that engineers can gain from the

* Corresponding author.
E-mail addresses: nijunjun@seu.edu.cn (J. Ni)

https://doi.org/10.1016/j.bgtech.2024.100158
Received 13 November 2024; Received in revised form 10 December 2024; Accepted 17 December 2024
Available online 20 December 2024

biological world to benefit geotechnical construction. By correlating ecological and geotechnical processes, overall sustainability can be achieved.

The atmosphere–plant–soil interaction is the key in eco-geotechnics, as climate change directly impacts atmospheric conditions, causing various plant species and soil types to behave differently. Plants can not only provide root mechanical reinforcement via root tensile strength but also contribute hydrologically to slope stability and erosion resistance. Plant transpiration–induced soil suction can increase the shear strength of soil and reduce the permeability of water, thus significantly affecting rainfall water infiltration in unsaturated soil slopes. When evaluating the stability of vegetated slopes under climate change, most studies have primarily focused on the behaviour of bare slopes under environmental loads, neglecting the effect of vegetation on the slope surface (Kim et al., 2017; Löbmann et al., 2020). Hence, understanding the effects of temperature, humidity, and plant roots on the behaviour of vegetated soil is essential for evaluating the stability of vegetated slopes under climate change (Ni et al., 2024). Existing literature has extensively explored the thermo-mechanical or hydro-mechanical modelling of bare unsaturated soils considering the effects of temperature and suction on yield surface and critical state (Tang & Cui, 2009; Xiong et al., 2016). To date, however, very few constitutive models have been developed that can describe the hydro-mechanical behaviour of root-permeated soils (Świtała & Wu, 2018; Woodman et al., 2020). Although the effects of plant roots on the hydraulic properties of soil, including soil water retention curves and water permeability, have been investigated through experimental and theoretical modelling (Ni et al., 2019a), these effects have yet to be incorporated into constitutive models of vegetated soils. Thus, the development of an advanced constitutive model that can simulate the thermo-hydro-mechanical behaviour of unsaturated vegetated soils is necessary.

This paper aims to provide a comprehensive review of recent advancements in eco-geotechnics and propose future research directions. Firstly, a unified framework for the atmosphere–plant–soil interaction is reviewed, including a novel eco-unsaturated soil constitutive model. Secondly, hydro-mechanical testing of vegetated soils along with model validation is discussed. Then, based on the theory and test results, some applications of eco-geotechnics are illustrated, such as slope stabilisation, the design of earthen landfill covers, and the cultivation of Chinese medicinal plants. Finally, the existing knowledge gaps and potential research directions in eco-geotechnics under climate change are highlighted. It should be noted that Ng et al. (2022a) mainly focused on reviewing several traditional frameworks for modelling atmosphere-plant-soil interactions. Nevertheless, this paper introduces the state-of-the-art constitutive model for unsaturated vegetated soil, which is also the first state-dependent model for vegetated soil.

2. Unified framework for atmosphere–plant–soil interactions

2.1. State-dependent unsaturated soil model

The key problems in unsaturated soil mechanics are related to the seepage, deformation, and failure caused by changes in the water content and stress state of the soil. Various constitutive variables have been proposed to model the mechanical behaviour of unsaturated soils (e.g., Wheeler et al., 2003; Russell & Khalili, 2006; Duan et al., 2019). Gens et al. (2006), who reviewed the different variables adopted in existing elastoplastic models, believed that '*Different constitutive stresses stand on an equal footing and the matter of adopting one or the other must be decided using the criteria of convenience*'. In the unified and state-dependent theoretical framework presented herein, net stress and matric suction are used for simplicity. Net stress is defined as the difference between total stress (σ) and pore air pressure (u_a), while matric suction represents the difference between pore air pressure and pore water pressure (u_w); hereinafter, it is referred to as suction for simplicity.

Based on net stress and suction, the constitutive formulations for an unsaturated soil can be expressed in the following general incremental form (Ng et al., 2020a):

$$\begin{bmatrix} \mathrm{d}\varepsilon_v \\ \mathrm{d}\varepsilon_q \\ \mathrm{d}S_r \end{bmatrix} = \begin{bmatrix} I_{11} & I_{12} & I_{13} \\ I_{21} & I_{22} & I_{23} \\ I_{31} & I_{32} & I_{33} \end{bmatrix} \begin{bmatrix} \mathrm{d}p \\ \mathrm{d}q \\ \mathrm{d}s \end{bmatrix}, \tag{1}$$

where $\mathrm{d}\varepsilon_v$ is the increment in volumetric strain; $\mathrm{d}\varepsilon_q$ is the increment in deviator strain; $\mathrm{d}S_r$ is the increment in the degree of saturation; $\mathrm{d}p$ is the increment in the mean net stress; $\mathrm{d}q$ is the increment in the deviator stress; $\mathrm{d}s$ is the increment in suction; and I_{ij} (i = 1, 2, and 3; j = 1, 2, and 3) are state-dependent variables for a given soil. According to Eq. (1), the variables I_{11}, I_{21}, and I_{31} in the compliance matrix describe the behaviour of unsaturated soils during compression, including the development of volumetric strain, deviator strain and the degree of saturation. Similarly, I_{12}, I_{22}, and I_{32} describe the hydro-mechanical behaviour during the shearing process, while I_{13}, I_{23}, and I_{33} reflect the behaviour of soil subjected to drying/wetting. All nine variables can be calibrated through suction-controlled and stress-controlled tests on unsaturated soils. These variables can also be determined using constitutive formulations for the compression, shearing, and water-retention behaviours of unsaturated soils, as discussed subsequently. Eq. (1) remains valid for saturated soil as well, which is considered a special case of unsaturated soil, with S_r = 100%. Under this special condition, net stress is replaced by Terzaghi's effective stress, and the values of I_{13}, I_{23}, I_{31}, I_{32} and I_{33} become zero.

The nine state variables within the stiffness matrix play important roles in Eq. (1). Understanding the coupling effects of suction and stress on these variables is crucial for advancing unsaturated soil mechanics theory and experimental research. The formulations of all nine terms in Eq. (1) are briefly discussed below; the details of their derivations have been provided by Ng et al. (2020a).

The variable I_{11} in Eq. (1) can be expressed as follows based on the assumption that the compression behaviour of an unsaturated soil can be described by a straight line in the e–ln p plane (Chiu & Ng, 2003):

$$I_{11} = \frac{\alpha_p(\mathrm{s})}{(1+e)p} \tag{2}$$

where e is the void ratio, and α_p(s) is the compressibility, which is a function of suction. Eq. (2) clearly reveals that the value of I_{11} is affected by the net stress, suction, and void ratio. The state-dependent compressibility is considered in this equation and hence in Eq. (1) as well.

The variable I_{12} in Eq. (1) can be derived based on the dilatancy formulation. In line with the state-dependent dilatancy proposed by Chiu and Ng (2003), I_{12} is determined as follows:

$$I_{12} = (I_{22} - 1/G_0)\mathrm{d}_1(s)\left(\exp(m\psi) - \frac{\eta}{M}\right) \tag{3}$$

where G_0 is the elastic shear modulus; $d_1(s)$ and m are material parameters, with the former being a function of suction; ψ is the state parameter (Chiu & Ng, 2003; Been & Jefferies, 1985); M is the gradient of the critical state line (CSL); and η is the stress ratio (q/p'). According to Eq. (3), the value of I_{12} is affected by suction. Therefore, the state-dependent dilatancy of unsaturated soils is considered in this equation and hence in Eq. (1) as well.

Using the equation proposed by Sheng et al. (2008), the variable I_{13} in Eq. (1) can be derived by calculating the suction-induced volume change of unsaturated soils:

$$I_{13} = \frac{\lambda_s}{(1+e)(p+s)} \tag{4}$$

where λ_s is the shrinkage index. A key feature of Eq. (4) is that the suction-induced volume changes of unsaturated soils are dependent on the mean net stress. The coupling effects of hydro-mechanical behaviour are also considered.

The variable I_{21} in Eq. (1) is mainly affected by the dilatancy during compression. Using the dilatancy equation presented by Chiu and Ng (2003), I_{21} can be determined as follows:

$$I_{21} = \frac{I_{11} - \kappa(s)/p}{(\lambda(s) - \kappa(s))\mathrm{d}_2(s)M/\eta} \tag{5}$$

where $\kappa(s)$ is the swelling index, and $\mathrm{d}_2(s)$ is a material parameter that depends on suction. Thus, the value of I_{21} is affected by suction. Therefore, the state-dependent dilatancy of unsaturated soils is considered in Eq. (5) and hence in Eq. (1) as well.

The value of I_{22} depends on the current deviator strain (ε_q). When ε_q is lower than the elastic threshold strain (ε_qe), the shear modulus is constant, and I_{22} can be calculated using the equation proposed by Ng and Yung (2008):

$$I_{22} = \frac{1}{C^2 f(\mathrm{e})\left(\frac{p}{p_\mathrm{r}}\right)^{2n}\left(1+\frac{s}{p_\mathrm{r}}\right)^{2k}} \tag{6a}$$

where C, n, and k are material parameters; $f(e)$ is the void ratio function relating the dependence of the shear wave velocity to the void ratio; and p_r is a reference pressure.

When the ε_q exceeds ε_qe, the strain dependence of the shear modulus should be considered. If the formulation presented by Vardanega and Bolton (2013) is used to model the strain-dependency of shear stiffness, I_{22} can be calculated using the following equation:

$$I_{22} = \frac{1+\left(\frac{\varepsilon_\mathrm{q}-\varepsilon_\mathrm{qe}}{\varepsilon_\mathrm{qref}-\varepsilon_\mathrm{qe}}\right)^{a}}{C^2 f(e)\left(\frac{p}{p_\mathrm{r}}\right)^{2n}\left(1+\frac{s}{p_\mathrm{r}}\right)^{2k}} \tag{6b}$$

where $\varepsilon_\mathrm{qref}$ is a characteristic reference strain, defined as the deviator strain at which the secant shear modulus is reduced to $0.5G_0$; α is a material parameter.

The variable I_{23} in Eq. (1) can be calculated as

$$I_{23} = \frac{I_{13}}{D_\mathrm{s}} - \frac{\alpha_\mathrm{s}}{D_\mathrm{s}(p+s)(1+e)} \tag{7}$$

where D_s is the dilatancy during drying/wetting. Eq. (7) implies that I_{23} is a function of I_{13}, α_s, and D_s, based on the foregoing discussion. Hence, the value of I_{23} can be readily calculated using this approach.

I_{31}, I_{32}, and I_{33} are all governed by the stress-dependent water retention behaviour. The water retention model developed by Zhou and Ng (2014) is used to derive these variables. The variable I_{31} in Eq. (1) can be determined as follows:

$$I_{31} = \frac{\partial S_\mathrm{r}}{\partial e}(1+e)I_{11} + \frac{\partial S_\mathrm{r}}{\partial \xi_m}\frac{\partial \xi_m}{\partial p} \tag{8}$$

where ξ_m is the ratio of the volume of micro-pores (V_M) to the total volume of pores (V_T), which characterises the pore size distribution (PSD).

The variable I_{32} in Eq. (1) can be determined using the following equation:

$$I_{32} = \frac{\partial\left[1+\left(s\frac{e^{m_4}}{m_3}\left(\frac{\xi_\mathrm{m}}{\xi_0}\right)^{-m_\mathrm{m}}\right)^{m_2}\right]^{-m_1}}{\partial e} D_\mathrm{q}(1+e)I_{22} \tag{9}$$

where ξ_0 is the initial value of ξ_m before any net stress has been applied; m_1, m_2, m_3, m_4, and m_m are the model parameters; and D_q is the dilatancy associated with the plastic mechanism of shearing. Eq. (9) indicates that the value of I_{32} is affected by several factors, including the effects of density on the soil water retention curve (SWRC), D_q, and I_{22}. As ample data is available in the literature for determining each of these parameters, I_{32} can be readily determined based on experimental results.

The variable I_{33} in Eq. (1) can be calculated using the following equation:

$$I_{33} = \frac{\partial\left[1+\left(s\frac{e^{m_4}}{m_3}\left(\frac{\xi_\mathrm{m}}{\xi_0}\right)^{-m_\mathrm{m}}\right)^{m_2}\right]^{-m_1}}{\partial s} \tag{10}$$

Notably, the value of I_{33} is not constant but depends on suction and stress. Moreover, the influence of stress on I_{33} is related to changes in the average void ratio and PSD.

2.2. Extended eco-unsaturated model for vegetated soils

Based on the unified framework expressed in Eq. (1), this section presents an extended eco-unsaturated model for vegetated soils. For brevity, only the key concepts and formulations are presented herein. Further details have been provided by Ng et al. (2024a) and Zhang (2024). The extended expression for unsaturated vegetated soil is as follows:

$$\begin{bmatrix}\mathrm{d}\varepsilon_\mathrm{v}\\ \mathrm{d}\varepsilon_\mathrm{q}\\ \mathrm{d}S_\mathrm{r}\end{bmatrix} = \begin{bmatrix}I'_{11} & I'_{12} & I'_{13}\\ I'_{21} & I'_{22} & I'_{23}\\ I'_{31} & I'_{32} & I'_{33}\end{bmatrix}\begin{bmatrix}\mathrm{d}p^*\\ \mathrm{d}q\\ \mathrm{d}s\end{bmatrix} + \begin{bmatrix}I'_{14}\\ I'_{24}\\ I'_{34}\end{bmatrix}[\mathrm{d}R_\mathrm{v}] \tag{11}$$

where R_v is the root volume ratio. The components of incremental strain induced by mechanical loading can be readily determined using Eqs. (2)–(10). However, even though these equations can be adopted, the root volume ratio (R_v) can affect the values of the parameters in these equations.

In the extended model, the normally consolidated line (NCL) and CSL depend on R_v.

$$\mathrm{NCL}(v - \ln p^* \text{ plane}):\ v = N(\xi) - \lambda(\xi)\ln\left(\frac{p^*}{p_\mathrm{ref}}\right) + \chi(R_\mathrm{v}) + \omega(R_\mathrm{v}) \tag{12}$$

$$\mathrm{CSL}(v - \ln p^* \text{ plane}):\ v = \Gamma(\xi) - \lambda(\xi)\ln\left(\frac{p^*}{p_\mathrm{ref}}\right) + \chi(R_\mathrm{v}) \tag{13}$$

$$\mathrm{CSL}(p^* - q \text{ plane}):\ q = M(R_\mathrm{v})p^* \tag{14}$$

where ξ is a state parameter describing the stabilising forces arising from the water meniscus, which is determined by suction and the degree of saturation (Gallipoli et al., 2003a); $N(\xi)$ and $\Gamma(\xi)$ are the intercepts of the NCL and CSL, respectively, on the $v - \ln p^*$ plane; and $\lambda(\xi)$ is the slope of these lines.

The shift in the NCL and CSL due to pore occupancy by plant roots is represented by the term χ in Eqs. (12) and (13), which is determined as follows:

$$\chi = b_r[1 - \exp(-bR_\mathrm{v})] \tag{15}$$

where b_r and b are parameters that describe the shift in the NCL due to pore occupancy.

Plant roots penetrate into soil pores and wrap around soil particles, contributing to the formation of aggregates within vegetated soil in addition to occupying pores (Hao et al., 2020). Apart from the physical interaction, biological and chemical interactions, exemplified by root exudates or mycorrhiza, can amplify soil aggregation in the rhizosphere (Albalasmeh & Ghezzehei., 2014; Bast et al., 2014). The bonding effects of these interactions are represented by an additional shift in the NCL (i.e., ω in Eq. (12)), which can be determined as follows:

$$\omega_0 = c\chi_0, \tag{16}$$

$$\mathrm{d}\omega = \omega\left(-\delta\sqrt{\mathrm{d}\varepsilon_v^{p2} + \mathrm{d}\varepsilon_s^{p2}} + \frac{\mathrm{d}\chi}{\chi}\right) \tag{17}$$

where c is a parameter that describes the contribution of the root tensile strength, χ_0 is the initial shift in the NCL due to pore occupancy, and δ is a degradation factor related to root breakage.

The dependence of the critical-state stress ratio on the root volume ratio can be expressed as follows:

$$M = M_0(1 + b_\mathrm{m}R_\mathrm{v}) \tag{18}$$

where M_0 is the critical state stress ratio of bare soil, and b_m is a parameter that describes the effects of roots on the critical state stress ratio.

Additionally, the bounding surface plasticity (Dafalias, 1986) is adopted to capture elasto-plastic behaviour. For a given suction and root volume ratio, the bounding surface can be expressed as

$$F_b = \left[\frac{q}{M(p^* + p_b)}\right]^n + \frac{\ln\left[\frac{p^* + p_b}{p_0(\xi, R_v) + p_b}\right]}{\ln r}, \tag{19}$$

where n and r are material parameters that describe the shape of the bounding surface; $p_0(\xi,\ R_v)$ is the pre-consolidation pressure of soil at the given suction and root volume ratio; and p_b is the bonding stress needed to enhance soil tensile strength, defined as $p_b = p_{b0}\omega$.

The incremental volumetric and deviatoric strain can be determined based on the bounding surface plasticity theory. Accordingly, the new items related to compression and shearing in Eq. (11) can be determined as

$$I'_{14} = \frac{d_1}{\eta}\left[M\exp(n_d\psi)\left(\frac{\rho}{\bar{\rho}_b}\right)^{\beta_D} - \eta\right]I'_{24} \tag{20}$$

$$I'_{24} = \frac{1}{K_p}\left[\frac{\partial F_b}{\partial M}\frac{\partial M}{\partial R_v} + \frac{\partial F_b}{\partial p_0}\frac{\partial p_0}{\partial \chi}\frac{\partial \chi}{\partial R_v} + \frac{\omega}{\chi}\left(\frac{\partial F_b}{\partial p_0}\frac{\partial p_0}{\partial \omega} + \frac{\partial F_b}{\partial p_b}\frac{\partial p_b}{\partial \omega} + \frac{\partial F_b}{\partial r}\frac{\partial r}{\partial \omega}\right)\frac{\partial \chi}{\partial R_v}\right] \tag{21}$$

where d_1, n_d, and β_D are material parameters related to soil dilatancy; $\frac{\rho}{\bar{\rho}_b}$ is the mapping ratio derived from bounding surface plasticity, which accounts for soil history; and K_p is the plastic modulus. The partial differentials in Eq. (21) can be derived from Eqs. (15)–(19).

Ng et al. (2016a) proposed a simple SWRC model for root-permeated soil, which assumes that plant roots occupy some soil pore space and thus reduce soil pore size. The void ratio of a root-permeated soil can be expressed as

$$e_{hy} = \frac{e_0 - R_v(1 + e_0)}{1 + R_v(1 + e_0)} \tag{22}$$

where e_0 is the void ratio of bare soil. $R_v = 0$ signifies the absence of plant roots in the soil (i.e., bare soil). Depending on the plant type, R_v can be a function of depth within the root zone. For water retention, only the unoccupied soil pores contribute to the air entry value (AEV). Thus, the void ratio in Eq. (22) is defined as the ratio of the volumes of unoccupied voids and solids (including soil particles and plant roots). Specifically, the volume occupied by roots is 'attached' to the solid soil particles when modelling the effects of roots on soil water retention. While describing state-dependent mechanical behaviour of vegetated soil, e_{me} (i.e., the ratio between total void volume and soil particle volume) is adopted as stress mainly transfers through soil skeleton. Therefore, to ensure compatibility, a relation between and e_{hy} in Eq. (22) can be established from the phase diagram of unsaturated vegetated soil:

$$e_{hy} = \frac{1 + e_{me}}{1 + R_v(1 + e_{me})} \tag{23}$$

To model the effects of the presence of roots on the change in the water retention ability of a soil, the void ratio–dependent SWRC equation proposed by Gallipoli et al. (2003b) can be adopted:

$$S_r = \left\{1 + \left(s\frac{\left[\frac{1 + e_{me}}{1 + R_v(1 + e_{me})}\right]^{m_4}}{m_3}\right)^{m_2}\right\}^{-m_1} \tag{24}$$

where m_1, m_2, m_3, and m_4 are the model parameters. As the void ratio has a negligible effect on the SWRC at high suction values, the product $m_1m_2m_4$ can be set to 1 (Gallipoli et al., 2003b). The Eq. (24) presents the formulation of main wetting or drying curves, characterised by two sets of model parameters. To capture the hysteretic behaviour of unsaturated soil, bounding surface plasticity can be employed. Two main curves act as bounding surfaces, with soil hydraulic states lying between them. A mapping rule incorporating suction history and current hydraulic state is required to obtain the plastic change in saturation along the scanning curves (Li, 2005).

Therefore, the variable I_{34} in Eq. (11) can be calculated using the following equation:

$$I'_{34} = \frac{\partial\left\{1 + \left(s\frac{\left[\frac{1 + e}{1 + R_v(1 + e)}\right]^{m_4}}{m_3}\left(\frac{\xi_m}{\xi_0}\right)^{-m_m}\right)^{m_2}\right\}^{-m_1}}{\partial R_v}. \tag{25}$$

In this newly developed eco-unsaturated model, root-induced hardening due to pore occupancy and internal bonding is modelled with dependence on the root volume ratio. As a result, it is the first state-dependent constitutive model for vegetated soil under unsaturated conditions. The development of this eco-unsaturated model enables researchers and engineers to investigate seasonal deterioration as well as failure mechanism of vegetated slopes subjected to extreme weather.

3. Experimental testing of the hydromechanical properties of vegetated soils

3.1. Hydrological properties

3.1.1. Water retention curve

The hydrological effects of vegetation extend beyond the antecedent effects of plant evapotranspiration (ET)–induced matric suction. Recent studies suggest that the presence of plant roots in soil can directly impact the hydraulic properties of soil (Li & Ghodrati, 1994; Scholl et al., 2014; Vergani & Graf, 2016; Ng et al., 2016a). Experimental work by Scanlan and Hinz (2010), Scholl et al. (2014), and Leung et al. (2015a) has shown that the presence of roots affects the water retention capacity of soil, particularly at low suction values, thus altering the SWRC. Field and laboratory tests (Gabr et al., 1995; Huat et al., 2006; Aravena et al., 2011; Ng et al., 2014a; Leung et al., 2015b) have demonstrated that vegetated soil has a lower water infiltration rate and a higher water retention capability than bare soil does. Changes in the hydraulic properties of soil due to roots can be attributed to the alteration in soil structure caused by roots occupying soil pore spaces (Scanlan & Hinz, 2010; Scholl et al., 2014; Leung et al., 2015a), which leads to changes in soil pore size and the SWRC (Romero et al., 1999; Ng & Pang, 2000; Ng & Leung, 2012).

The SWRC is a vital parameter controlling plant growth in vegetated soils (Clarke & Townley-Smith, 1986). In agricultural science, determining the SWRC is crucial for planning irrigation schemes and assessing the water use efficiency of plants (Shwetha & Varija, 2015). Fig. 1A compares the SWRCs of bare and vegetated soils (Leung et al., 2015a), which were fitted using the van Genuchten (1980). The curves show that the AEV of vegetated soils is consistently approximately 3–4 kPa higher than that of bare soil in both drying and wetting paths. However, the desorption rate does not vary significantly. Similar changes in SWRC due to root presence are observed in the test data presented by Rahardjo et al. (2014) and Yan and Zhang (2015). The measured and predicted increments in AEV both indicate an increase in water retention capability due to roots occupying soil pore spaces. This finding concurs with the experimental observations of Romero et al. (1999) and Ng and Pang (2000), which indicates that bare soil with a low void ratio (i.e., denser soil) would possess a higher AEV.

Fig. 1B–D show the measured SWRCs of bare soil tested in the aforementioned studies. Each SWRC is fitted with Eq. (24) to calibrate the coefficients m_1, m_2, m_3, and m_4. Based on these coefficients and the root parameter R_v, the SWRC of root-permeated soil was predicted and compared with the respective measurements (including all replicates). The measurements and predictions generally agree well in all three cases, with the maximum discrepancy in S_r being less than 13 % at any given suction. The presence of roots consistently caused an increase in AEV, while the desorption rate did not change significantly in any of the cases. Similar changes in SWRC due to root presence are observed in the

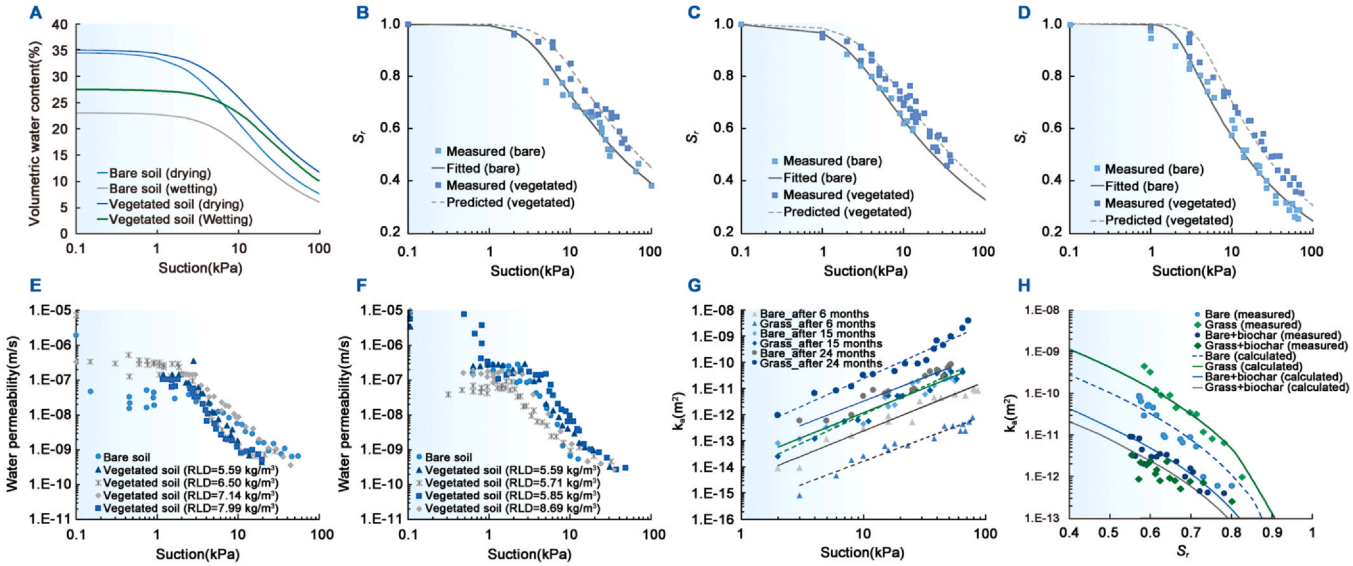

Fig. 1. (**A**) SWRC of vegetated soils (Leung et al., 2015a); Comparison of measured and predicted SWRCs of bare and vegetated soil from (**B**) the field tests conducted by Ng et al. (2016a), (**C**) the laboratory tests conducted by Ng et al. (2016b), and (**D**) the laboratory tests reported by Leung et al. (2015a); Measured effects of plant roots on $k(\psi)$ for (**E**) silt and (**F**) clayey sand (Jotisankasa & Sirirattanachat, 2017); (**G**) Air permeability function in bare and grass-covered soils (Ni & Ng, 2019); (**H**) Comparison between measured and calculated air permeability functions for vegetated soil subjected to biochar treatments (Ni et al., 2023).

test data presented by Rahardjo et al. (2014) and Yan and Zhang (2015). The measured and predicted increments in AEV both indicate an increase in water retention capability due to roots occupying soil pore spaces. This finding is consistent with experimental observations reported by Romero et al. (1999) and Ng and Pang (2000), who also found that denser soil with a lower void ratio would exhibit a higher AEV.

3.1.2. Water permeability function

Soil water permeability is another key hydraulic parameter for analysing water infiltration in both saturated and unsaturated soils. The presence of plant roots can cause saturated water permeability (k_s) to vary from −143 % to 1085 %. Actively growing young roots reduce k_s due to pore clogging, whereas decaying roots of mature plants may increase k_s. Tree/shrub species induce the largest changes in k_s in coarse-textured soil, followed by grass and crop species. Apart from plant type, plant ageing affects k_s significantly. Leung et al. (2017) reported that the growth of plant roots, i.e., an increase in root length density (RLD), causes a linear increase in k_s. Ng et al. (2020b) observed a bilinear relationship between k_s and RLD, whereby k_s initially decreases with increasing RLD and then increases when RLD surpasses a threshold value. Other studies (e.g., Lu et al., 2020) have revealed that changes in k_s are proportional to variations in root diameter.

Root-induced changes in unsaturated water permeability ($k(\psi)$) also depend on root characteristics at various growing periods. Song et al. (2017) reported that the fibrous root system in grass species reduces $k(\psi)$ by blocking soil pore space, whereas tap root systems increase k by creating preferential flow paths. Wahren et al. (2009) found that the $k(\psi)$ in forest sites can be 2–4 times that in cropland sites. Jotisankasa and Sirirattanachat (2017) adopted the instantaneous profile method in laboratory studies to measure the effects of roots on $k(\psi)$ for two types of soil with varying root contents (Fig. 1C and 1D). Root-induced changes in $k(\psi)$ were prominent mainly for matric suction values below 10 kPa. The test data also suggest that plant roots do not necessarily reduce water permeability. Interestingly, one of the vegetated soil samples, with an RLD of 5.85 kg/m^3, exhibited dual-permeability behaviour (Fig. 1D). When the matric suction was below 1 kPa, its water permeability was up to two orders of magnitude higher than that of bare soil. Thus, whether the presence of plant roots would increase or reduce water permeability remains unclear. Some field and laboratory studies (Gish & Jury, 1983; Gabr et al., 1995; Ng et al., 2014a; Rahardjo et al., 2014) have shown a reduction in water permeability, whereas others have revealed an increase in water permeability due to decayed roots (Li & Ghodrati, 1994; Vergani & Graf, 2016) or competition for resources (Ng et al., 2016b; Ni et al., 2017, 2018b). Recent modelling efforts by Shao et al. (2017) have shown that a dual-permeability model could capture the hydrological responses of vegetated soils better than the conventional single-permeability model.

3.1.3. Air permeability function

Plant roots are crucial in determining the total porosity, pore size, and pore continuity of vegetated soil, which, in turn, affect soil air permeability. Cai et al. (2010) have shown that vegetation root systems increase the air permeability of soil, which causes vegetated soil to produce a higher gas flux than bare soil. Different plant species affect the air permeability of soil differently (Chen et al., 2014). For instance, forage radish and rapeseed induce the highest air permeability under high compaction, while rapeseed and rye increase air permeability the most under no compaction. This difference arises because species such as forage radish and rapeseed can grow roots into compacted soil, unlike other species such as rye. Additionally, soil texture is important in governing the effects of roots on air permeability. The pore continuity of clayey soil is improved by the presence of root channels, leading to increased air permeability. However, in sandy and granular soils, air permeability is influenced less by pore continuity (Chen et al., 2014). Plant age is another factor affecting the root-induced alteration of air permeability.

Ni and Ng (2019) observed that after six months of plant growth, the air permeability of grass-covered soil was lower than that of bare soil (Fig. 1G). In contrast, the air permeability of grass-covered soil exceeded that of bare soil after 15 months of plant growth. The reduction in air permeability due to vegetation in the early stage was attributed to the occupancy of soil pores and the blockage of flow channels by plant roots. However, the plants increased the air permeability of the soil after a relatively long period of growth because the root decay created preferential channels and enhanced the gas migration through the soil (Ni & Ng, 2019). Moreover, Ni et al. (2023) investigated the effects of biochar on air permeability changes in a plant–soil system (Fig. 1H). Compared with bare soil, grass-covered soil and a biochar-treated grass group exhibited higher and lower air permeability, respectively. This

was because when biochar was absent, the decayed roots in the grass-covered soil induced an increase in air permeability at all soil moisture levels. However, peanut shell biochar reduced the rate of root decay and preserved the water retention capacity, leading to a reduced air permeability (Ni et al., 2023).

3.2. Mechanical properties

3.2.1. Root biomechanical properties

The biomechanical properties of roots are pivotal in the context of soil reinforcement and slope stability. Boldrin et al. (2018) investigated the effects of root dehydration on the biomechanical properties of the woody roots of *Ulex europaeus*. As shown in Fig. 2A and B, the tensile strength and Young's modulus of the roots increased significantly when the root moisture content decreased below 0.5 g/g. After 30 days of burial in dry soil, the tensile strength and Young's modulus of the roots increased significantly; however, no significant change was observed in wet soil. The biomechanical properties of roots can vary among plant species, including *Populus tomentosa*, *Robinia pseudoacacia*, and *Olea europaea* (Wang et al., 2019). The tensile strength decreases as the root diameter increases, following a distinct power law equation for each species. The mean tensile strength of *R. pseudoacacia* exceeds that of *P. tomentosa* and *O. europaea*. Hence, due to greater additional root cohesion, the root systems of *R. pseudoacacia* provide a significantly higher improvement in the factor of safety (FOS) for a slope than those of *P. tomentosa* or *O. europaea* do. Additionally, Lee et al. (2023) have shown the importance of selecting plant species based on their growth traits, root mechanical features, and resistance to wind erosion for sand dune restoration projects. Based on their results, the root pull resistances of *Canavalia lineata* and *Canavalia rosea* are significantly higher than that of *Vigna marina*, while the root tensile strength of *C. rosea* is significantly higher than that of *C. lineata* and *V. marina*. In wind tunnel tests, *C. lineata* showed better resistance to wind erosion than *C. rosea* and *V. marina*. Thus, strategies for either slope management or erosion control need to be designed considering the suitability of plant species.

The growth and decay of roots may affect the biomechanical reinforcement that they provide. As shown in Fig. 2C and D, Kamchoom et al. (2022) investigated how the tensile strength of fibrous roots is affected by different means of land clearance, such as burning and herbicide application. The researchers hypothesised that root age and the deposition of structural components, such as cellulose and lignin, contribute to an increase in root tensile strength. They also compared the effects of burning and herbicide application on root decay and tensile strength. The results indicate that older roots have higher cellulose and lignin contents and can thus provide greater tensile strength. Furthermore, the root decay caused by herbicide treatment reduces root tensile strength faster and more significantly than incineration treatment does, because the cellulose and lignin contents are reduced faster by herbicide treatment.

3.2.2. Shearing behaviour

The presence of roots significantly increases the shear yield stress and deformation energy of soil but has no significant effect on soil elasticity or residual stress (Ghestem et al., 2014). Residual stress depends more on the confining pressure and soil moisture (an inherent property of the soil) than on the presence of roots. Pallewattha et al. (2019) found that the presence of roots significantly increases the shear strength of soil. Through direct shear tests, they observed that soil samples with root penetration exhibited approximately 5–8 kPa higher shear strength than unreinforced samples. Soil suction (caused by plant transpiration) also influences the shear strength of soil–root systems considerably. Tests conducted at different suction levels showed an interdependence between root reinforcement and soil suction, especially at suction levels of 50 kPa and above, which increased the shear strength of the soil by over 15 kPa.

The density, branching, length, volume, inclination, and direction of root systems significantly affect the mechanical properties of soil. Both above and below the shear plane, the length or volume of thick roots and the branching density are critical for the formation of a dense root network. Ni et al. (2019b) investigated the influence of plant spacing on root tensile strength and soil shear strength in vegetated soils. They found that plant spacing does not significantly affect root cohesion, which quantifies the contribution of mechanical root reinforcement to soil shear strength. Foresta et al. (2020) conducted triaxial compression tests on intact vegetated silty sand with various root volume ratios

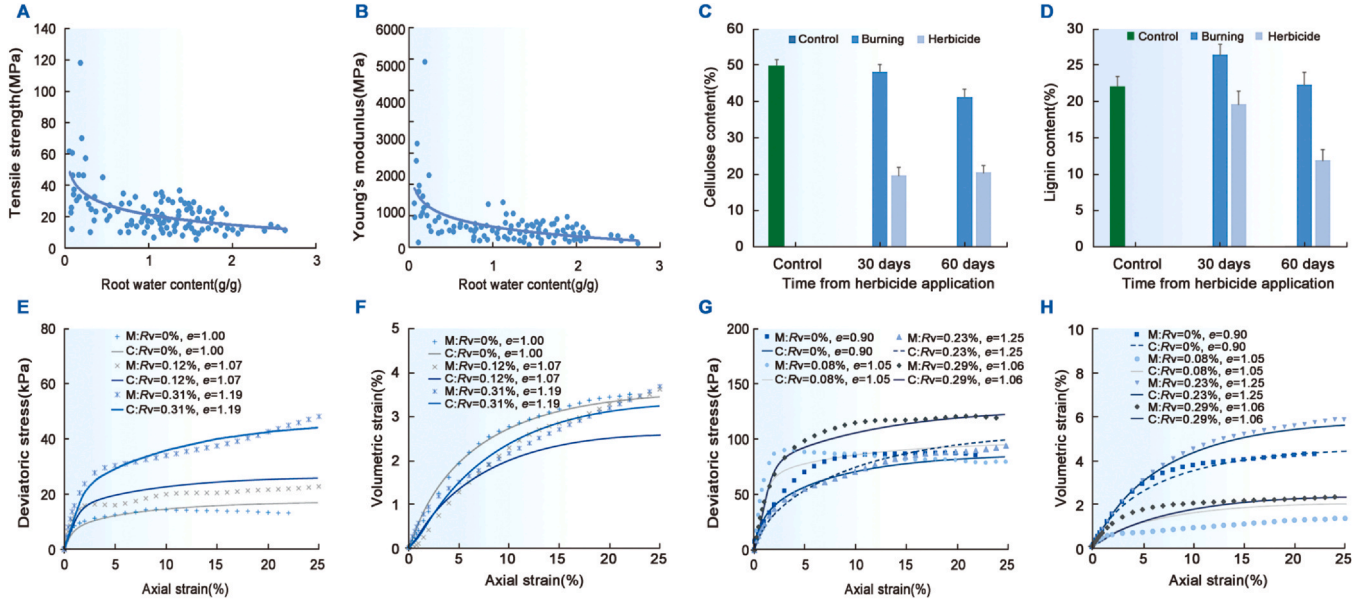

Fig. 2. (**A**) Root tensile strength and (**B**) Young's modulus plotted against root water content (Boldrin et al., 2018); (**C**) Mean cellulose content (± standard error) and (**D**) lignin content (± standard error) of *Cynodon dactylon* roots randomly sampled from planted soil columns at 30 and 60 days, compared between two grass-killing methods (Kamchoom et al., 2022); Effects of root volume ratio on shearing response of vegetated soil (Foresta et al., 2020; Ng et al., 2024a): (**E**) Deviatoric stress versus axial strain (p^* = 10 kPa), (**F**) Volumetric strain versus axial strain (p^* = 10 kPa), (**G**) Deviatoric stress versus axial strain (p^* = 30 kPa), (**H**) Volumetric strain versus axial strain (p^* = 30 kPa).

(Fig. 2E–H). The results computed by Ng et al. (2024a) using a newly developed constitutive model, as described in Section 2.2, are also presented. A clear trend is discernible in that the shear strength of vegetated soil is significantly higher than that of bare soil. Moreover, the state dependence of vegetated soil under shearing is visible in both the computed and measured results. Compared with bare soil having a void ratio of 0.90, two vegetated soils having slightly higher void ratios (1.05 and 1.06) showed less contractive behaviour. Conversely, another vegetated soil with a much larger void ratio exhibited a greater contractive tendency. The former behaviour is mainly governed by a higher root volume ratio, whereas the latter is predominantly controlled by the void ratio. In addition to root density, root morphology affects the shear strength of vegetated soil. Ghestem et al. (2014) found that *Ricinus communis* provided the greatest shear resistance due to its straight root system with many vertical roots. By comparison, *Jatropha curcas* has inclined and vertical roots that can create vulnerable areas in the soil profile, while *Rhus chinensis* has many horizontal lateral roots that are the least effective in providing shear resistance.

Kamchoom et al. (2022) specifically focused on the effects of root growth and decay, finding that the roots of *Cynodon dactylon* (Bermuda grass) significantly increased the soil shear strength after six months of growth. This is mainly attributable to the increase in cellulose content during root growth, which increases the tensile strength and modulus of the root system. After root decay is introduced by burning or herbicide application, the tensile properties of the roots are significantly weakened; this reduces the expansibility and shear strength of the soil, with the values falling even lower than those of fallow soil. Root decay caused by herbicide application is faster and more pronounced than that caused by incineration because herbicides cause more severe decay and greater damage to the biomechanical properties of roots. Root decay also reduces soil expansibility, rendering vegetated soils more contractile than fallow soils.

Previous studies have observed that root mechanical reinforcement plays a more significant role in slope stabilisation compared to root hydraulic reinforcement (Phillips & Watson, 1994; Sidle & Ochiai, 2007; Sidle & Bogaard, 2016; Lei et al., 2022). These conclusions are based on extensive field monitoring of slopes subjected to multiple wet-dry cycles, where pre-existing preferential flow paths were identified. Through these pathways, rainfall water can infiltrate into deeper soil layers, thereby weakening the effects of root hydraulic reinforcement. However, in artificial or natural slopes without such preferential flow paths, the contribution of hydraulic reinforcement to slope stability can be up to 120 % greater than that of mechanical reinforcement (Ng et al., 2016d). While the extent of this impact may vary, similar findings have been reported in numerous other studies (Pollen-Bankhead & Simon, 2010; Boldrin et al., 2021a, 2021b; Bordoni et al., 2024). Mixed plant species of different functional groups (e.g., tree and grass) are often found in the field, instead of single species (Somers & Asner, 2013; Ehrmann, & Ritz, 2014; Ng et al., 2020b). The 3D numerical model, developed by Ng et al. (2021), can be employed for simulating hydrological and mechanical reinforcements of different plant species. In their model, the primary and secondary roots are differentiated while modelling root hydro-mechanical reinforcements. Hence, both fibrous and tap root system for various plant species can be satisfactorily modelled. Additionally, the aging effects on soil water retention (Ni et al., 2019) and tensile strength (Boldrin et al., 2021) needs to be considered while considering long-term performance of vegetated soil.

4. Applications of eco-geotechnics

4.1. Slope stabilisation

Studies have predominantly focused on the mechanical reinforcement effect of plant roots, ignoring the more important hydraulic effect of vegetation. In light of this gap, based on state-dependent unsaturated soil mechanics, Ng (2017) proposed considering the hydraulic effect of vegetation with different root architectures, including two important aspects: (i) plant root water uptake due to transpiration and (ii) the permeability and water retention of vegetated soils. Traditional unsaturated soil mechanics theory does not consider the complex seepage–deformation–strength coupling effect in vegetated soil. Therefore, state-dependent unsaturated soil mechanics theory is crucial for analysing the scientific mechanism of vegetated slope protection and guiding relevant engineering practices.

4.1.1. Calculation method for seepage and stability of unsaturated vegetated soil slope

To quantify the effect of plant root water uptake on unsaturated soil, a sink term (S) is introduced into the Richards equation. To fill the gap in the theoretical model regarding how water uptake by differently shaped roots impacts soil pore water pressure, Ng et al. (2015a) and Liu et al. (2018) derived an analytical solution considering the influence of different root architectures ($G(z)$) on the sink term (S). Common root shapes include uniform (Feddes et al., 1978), triangular (Prasad, 1988), exponential (Raats, 1974), and parabolic (Leung et al., 2015b), the functions of which are as follows:

$$G(z)=\begin{cases}\frac{1}{L_2}, \text{ Uniform}\\ \frac{2}{L_2}\left(\frac{z-L_1}{L_2}\right), \text{ Triangular}\\ \frac{\exp(z-L_1)-1}{\exp(L_2)-L_2-1}, \text{ Exponential}\\ \frac{2}{L_2}\left[\frac{3(z-L_1)L_2-(z-L_1)^2}{L_2^2}\right], \text{ Parabolic}\end{cases} \tag{26}$$

where L_1 and L_2 are the vertical lengths of the rootless and rooted zones, respectively, and z is the vertical coordinate axis (positive upward). Considering a multi-layered vegetation slope, as shown in Fig. 3A, if the contour lines of pore water pressure are parallel to the slope surface, the seepage problem of the unsaturated slope can be simplified into a one-dimensional problem involving seepage perpendicular to the slope direction (Zhan et al., 2013). Furthermore, considering the influence of $G(z)$ on S, the transient analytical solution of the pore water pressure (u_w) for an unsaturated vegetated slope can be derived; the specific derivation process has been detailed by Ng et al. (2015a):

$$u_w=10\alpha^{-1}\ln\left\{k_0^*+8\frac{(\cos\beta)^2}{\theta_s-\theta_r}\exp\left[\frac{\alpha(L-z)\cos\beta}{2}\right]\cdot \sum_{n=1}^{\infty}\frac{\left(\lambda_n^2+\frac{\alpha^2}{4}\right)\sin(\lambda_n L\cos\beta)\sin(\lambda_n z\cos\beta)}{2\alpha+\alpha^2 L\cos\beta+4L\cos\beta\lambda_n^2}G(t)\right\} \tag{27}$$

where α is the soil desaturation coefficient; k_0^* is the steady-state analytical solution considering different root shapes; β is the slope inclination angle; θ_s and θ_r are the saturated and residual volumetric water contents, respectively; L is the total depth of the slope perpendicular to the slope surface (i.e., L_1+L_2); λ_n is the n^{th} positive root of the equation $\sin(\lambda L\cos\beta)+2\lambda\cos(\lambda L\cos\beta)/\alpha=0$; and $G(t)$ is a function related to the transient boundary conditions (Ng et al., 2015a). Considering both the mechanical reinforcement effect and the hydraulic effect of vegetation, Feng et al. (2020) further derived the FOS (F_s) for an unsaturated vegetated slope, which is expressed as follows:

$$F_s=\frac{c'+R_f T_r RAR-u_w\tan\varphi_b}{\left[\gamma_d(L-d)+\gamma_w\int_z^L\theta dz\right]\sin\beta\cos\beta}+\frac{\tan\varphi'}{\tan\beta} \tag{28}$$

where c' is the effective cohesion; R_f is the correction factor considering root orientation; T_r is the tensile strength of the roots; φ' is the critical friction angle; φ_b is the suction-related friction angle; γ_d and γ_w are the unit weights of dry soil and water, respectively; and θ is the volumetric water content of the soil. RAR is the root area ratio, defined as the total cross-sectional area

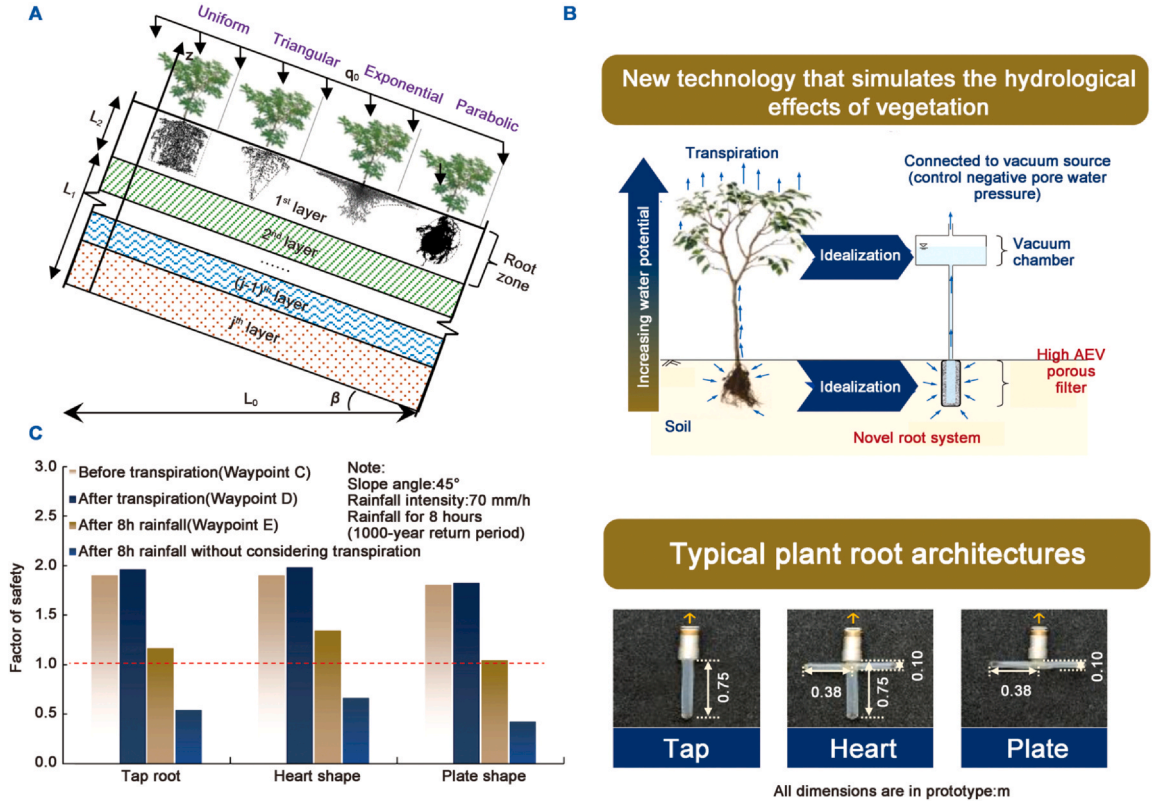

Fig. 3. (**A**) Schematic of a multi-layered slope with different root architectures (Feng et al., 2020); (**B**) Working principle of new artificial root along with three common root architectures (Ng et al., 2016d); (**C**) Effects of root architecture on the FOS of vegetated slopes (Ng et al., 2016d).

of all plant roots on a horizontal cross-section at a certain depth, divided by the total cross-sectional area of the soil at that depth (Ng, 2017).

The aforementioned analytical solution shows that the exponential root system generates the highest suction in the soil, followed by the triangular, uniform, and parabolic root systems (Ng et al., 2015a). Under steady-state drying, the maximum suction generated by the parabolic root system is approximately 77 % of that generated by the exponential root system. Additionally, the depth range of the vegetation root system affecting soil suction is approximately 3–6 times the root depth. In a multi-layered slope, as the permeability of the soil layer beneath the vegetation layer decreases, the root system can generate greater suction (Liu et al., 2018; Feng et al., 2019). Therefore, in engineering practice, higher degrees of compaction can be considered for the soil beneath the vegetation layer; this would reduce the permeability of the soil, enhancing the effect of root water uptake on the suction distribution and improving the slope stability through stress coupling.

The calculated results also demonstrate that when the mechanical and hydraulic reinforcement effects are coupled, the enhancement in the FOS for a slope with an exponential root system is about 130 % greater than that for a slope with a uniform root system. This indicates that the exponential root system influences slope stability more than the uniform root system (Feng et al., 2020). Importantly, the mechanical reinforcement effect of vegetation can improve the FOS for a slip surface only within the rooted zone, while the hydraulic effect can control the FOS in deeper zones as well. In summary, the analytical solution shown in Eqs. (27) and (28) provides an effective method for designing slope stability considering different vegetation types (root architectures) in practical engineering applications.

4.1.2. Centrifuge model tests of unsaturated vegetated soil slopes

The centrifuge test technique has been widely used to study various engineering problems (Ng, 2014). In recent years, to explore the interaction between vegetation and soil in the geotechnical centrifuge, detached plant roots (Sonnenberg et al., 2010) or plastic root models (Liang et al., 2017) have usually been employed. However, both techniques can only simulate the mechanical reinforcement effect of plant roots, ignoring the hydraulic effect of vegetation. Consequently, they cannot be used to study the coupling effect of suction state and stress state in vegetated soil and related geotechnical structures.

To address this issue, Ng et al. (2014b; 2016c) developed a new type of artificial root system that can simulate both the mechanical reinforcement and hydraulic effects of vegetation in the centrifuge. Fig. 3B shows the working principle of the new artificial root, which mainly comprises a hollow tube made of cellulose acetate. The cellulose acetate material has a high AEV (~100 kPa), which enables effective simulation of the hydraulic gradient formed by root water uptake. This material can also simulate the mechanical properties of plant roots, including elastic modulus, tensile strength, and root–soil contact friction angle. Fig. 3B also shows three representative root shapes (tap, heart, and plate), of which the tap and heart shapes are similar to uniform and exponential roots, respectively.

Ng et al. (2016d) conducted a series of centrifuge tests using the aforementioned artificial roots (tap-, heart-, and plate-shaped) to investigate the influence of root shape on suction distribution and on the stability of a 45° granite residual soil slope. The results showed that the slope reinforced with heart-shaped roots had the highest suction during heavy rainfall, indicating that this root shape provides the maximum hydraulic effect. Ng et al. (2016d) also performed numerical analysis based on the measured results (Fig. 3C). After 8 h of artificial rainfall, the FOS of the heart-shaped roots was approximately 16 % and 28 % higher than that of the tap and plate-shaped roots, respectively, and the FOS of all slopes remained above the safety threshold (i.e., 1.0); this is consistent with the observation that all slopes were stable after rainfall in the centrifuge tests. Leung et al. (2017) also found through centrifuge tests that heart-shaped roots were superior to tap roots in reinforcing a 60° granite residual soil slope. The difference is closely related to the suction generated by plant transpiration. Additionally, the FOS when considering only the

reinforcement effect without the hydraulic effect of vegetation (i.e., plant transpiration) is presented in C for comparison (Ng et al., 2016d). The FOS after 8 h of rainfall was below the safety threshold, which means that ignoring the hydraulic effect of vegetation and considering only the mechanical reinforcement effect would lead to an underestimation of the vegetated slope's stability. Based on theoretical model prediction and centrifuge test verification, the hydraulic effect of vegetation (i.e., root water uptake), which depends on the root shape, significantly increases slope stability. Therefore, in ecological slope protection and restoration projects, the appropriate root shape should be selected based on the hydraulic effect of vegetation to achieve better control over the suction state of unsaturated soil and improve slope stability.

4.2. Design of earthen cover system

Another important application of eco-geotechnical theory is the design of earthen landfill covers, which operate entirely in the unsaturated state. These landfill covers, acting as the 'skin' of municipal solid waste landfills, are designed mainly to prevent rainwater infiltration and landfill gas emission and thereby reduce leachate production. Modern landfills typically use low-permeability geosynthetic materials, such as geomembranes. However, under heavy rainfall, geomembranes are prone to instability at their interface with the soil. To satisfy the requirements for the humid climate regions in southern China and Hong Kong, which experience an annual rainfall of up to 2500 mm, Ng et al. (2015b) developed a vegetated three-layer soil cover system based on eco-geotechnical theory. This cover system comprises three layers, namely (from top to bottom) a water storage layer, a drainage layer, and a low-permeability layer, the material permeabilities of which are significantly influenced by the suction state.

4.2.1. Working principle of the three-layer cover system

Fig. 4A shows the conceptual diagram of the proposed three-layer landfill cover. The cover with capillary barrier (CCBE) system inhibits water infiltration through the capillary barrier effect produced by the contrasting permeabilities of its two soil layers. In the three-layer landfill cover system, a low-permeability soil layer is added underneath the CCBE. According to the water permeability functions illustrated in Fig. 4B, the water infiltration through the CCBE at the top is restricted by the low-permeability soil layer below, even under the low-suction conditions in humid climates. Conversely, under the high-suction conditions during dry seasons, the low water permeability of the CCBE protects the soil layer below from desiccation. The soils are relatively wet in humid weather and even close to being saturated under heavy rainfalls. However, rainfall infiltration reduces the soil suction in the cover system to values below S_1 (Fig. 4B). Thereby, the CCBE created by the fine-grained soil layer on top and the underlying coarse-grained soil layer loses its function, allowing water to infiltrate into the coarse-grained soil layer. Nevertheless, the infiltrating water is intercepted by the low-permeability soil layer at the bottom and is drained away through the coarse-grained soil layer (which has a relatively high saturated permeability). Therefore, water ponding on the low-permeability soil layer at the bottom is prevented. The working principles of this three-layer landfill cover system are detailed in a patent filed by Ng et al. (2015b).

The aforementioned cover system can be constructed entirely using recycled construction waste and engineering soil with appropriate particle sizes. The material properties can be controlled based on state-dependent unsaturated soil theory (Ng et al., 2019). This approach not only expands the potential reusability of solid waste materials, such as construction waste in China, but also enhances their utilisation rate. Additionally, it supports energy conservation and emission reduction efforts, contributing to the national goal of achieving carbon neutrality. Moreover, due to their aesthetic and ecological value, plants are often used for greening and ecological restoration of landfill cover systems. Landfill plants can occupy the soil pores in the cover system through root growth, improving the soil's water retention capacity. The water uptake capacity of these plants can also be regulated through the leaf area and root shape, which allows for controlling the suction state of the soil. Thus, this strategy further enhances water storage capacity as well as the capability to mitigate water infiltration and gas emission.

4.2.2. Long-term field performance

To investigate the field performance of the vegetated three-layer landfill cover system under humid climates, long-term field monitoring

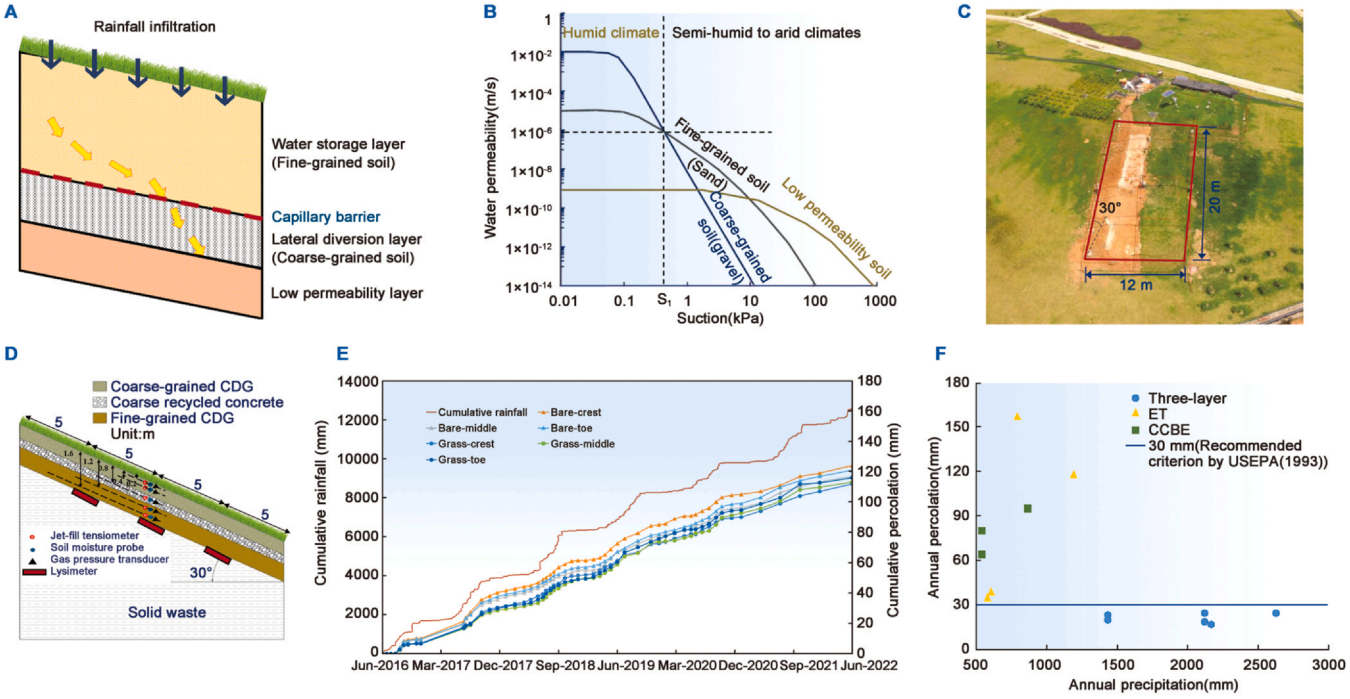

Fig. 4. (**A**) Schematic of proposed three-layer earthen landfill cover; (**B**) Water permeability functions of fine-grained, coarse-grained, and low-permeability soils (Ng et al., 2019); (**C**) Aerial view of the monitoring site at the Xiaping landfill, Shenzhen, China; (**D**) Cross-section showing the instrumentation plan (Ng et al., 2024b); (**E**) Measured cumulative percolation in the bare land and the vegetated three-layer landfill cover system for six years (Ng et al., 2024b); (**F**) Comparison of measured annual percolation among three landfill cover systems.

was conducted at the Xiaping landfill in Shenzhen, China (Ng et al., 2024b). As shown in Fig. 4C, the monitoring area was divided into two equally sized portions, each measuring 20 m in length and 6 m in width. One portion was planted with Bermuda grass for revegetation, while the other was left bare for comparison. The cover system comprised three soil layers (Fig. 4D), namely (from top to bottom) a 0.6 m layer of coarse-grained granite residual soil (coarse-grained CDG), a 0.4 m layer of coarse recycled concrete (CRC), and a 0.8 m layer of fine-grained CDG. Fig. 4E shows the changes in cumulative percolation measured using lysimeters at three locations (i.e., toe, middle, and crest) in both the bare and vegetated three-layer cover systems during the six-year field monitoring period (2016–2022). The total rainfall during the monitoring period exceeded 12,000 mm, with 80 % occurring in the rainy season from April to October each year. Compared with the bare cover, the vegetated cover reduced annual percolation by up to 22 % in the first two years of monitoring. This reduction is primarily due to the higher soil suction caused by vegetation, which reduces soil permeability (Scanlan., 2009). At the end of the monitoring period, the average annual percolation for the vegetated cover was measured to be approximately 19 mm. The measured maximum annual percolation values for both the bare and vegetated covers were lower than the design criterion (30 mm/yr) recommended by United States Environmental Protection Agency USEPA (1993). This demonstrates that even without a geomembrane, the three-layer landfill cover system minimises water infiltration and gas emissions effectively in humid climates.

Fig. 4F compares the measured annual percolation among three cover systems, namely the three-layer landfill cover system, an ET cover, and CCBE. The performance data for the ET and CCBE cover systems was sourced from previous studies conducted in humid regions of the USA (Nyhan et al., 1990; Warren et al., 1996; Karr et al., 1999; Albright et al., 2004) and Germany (Melchior, 1997). All ET covers reported in the literature are from the USA. The ratio of annual percolation to annual rainfall for CCBE was 11 %–15 %, while the measured annual percolation through the ET cover and CCBE was larger than 30 mm, even though the annual precipitation was only around 500 mm. The water permeability of the cover materials was likely not sufficiently low, even for the ET cover. With the CCBE, the fine-grained and coarse-grained soils could not provide sufficient contrast in water permeability. However, the annual percolation through the three-layer landfill cover system remained considerably lower than that through the ET cover or CCBE, even under annual precipitations exceeding 2600 mm. The measured annual percolation through the three-layer landfill cover system was less than 30 mm, meeting the design criterion recommended by the United States Environmental Protection Agency USEPA (1993). The six-year monitoring exercise demonstrated the effectiveness of the three-layer landfill cover system in minimising water percolation in humid climates, even without a geomembrane.

4.3. Cultivation of Chinese herb medicine

4.3.1. Soil conditioning for improved medicinal plant production and quality

Herbal medicines have become increasingly popular worldwide. The annual global market for herbal medicines grew from USD 83.1 billion in 2012 to approximately USD 110.2 billion in 2020 (WHO, 2013; GIA, 2022). This growth is expected to continue, with the market projected to reach USD 190.4 billion by 2027. The medicinal organ (root tuber) is a vital component of medicinal plants (Fig. 5A) as it contains active ingredients that possess high pharmaceutical value. The yield and quality of medicinal plants can be significantly impacted by the soil properties and atmospheric conditions. In China, the growth of

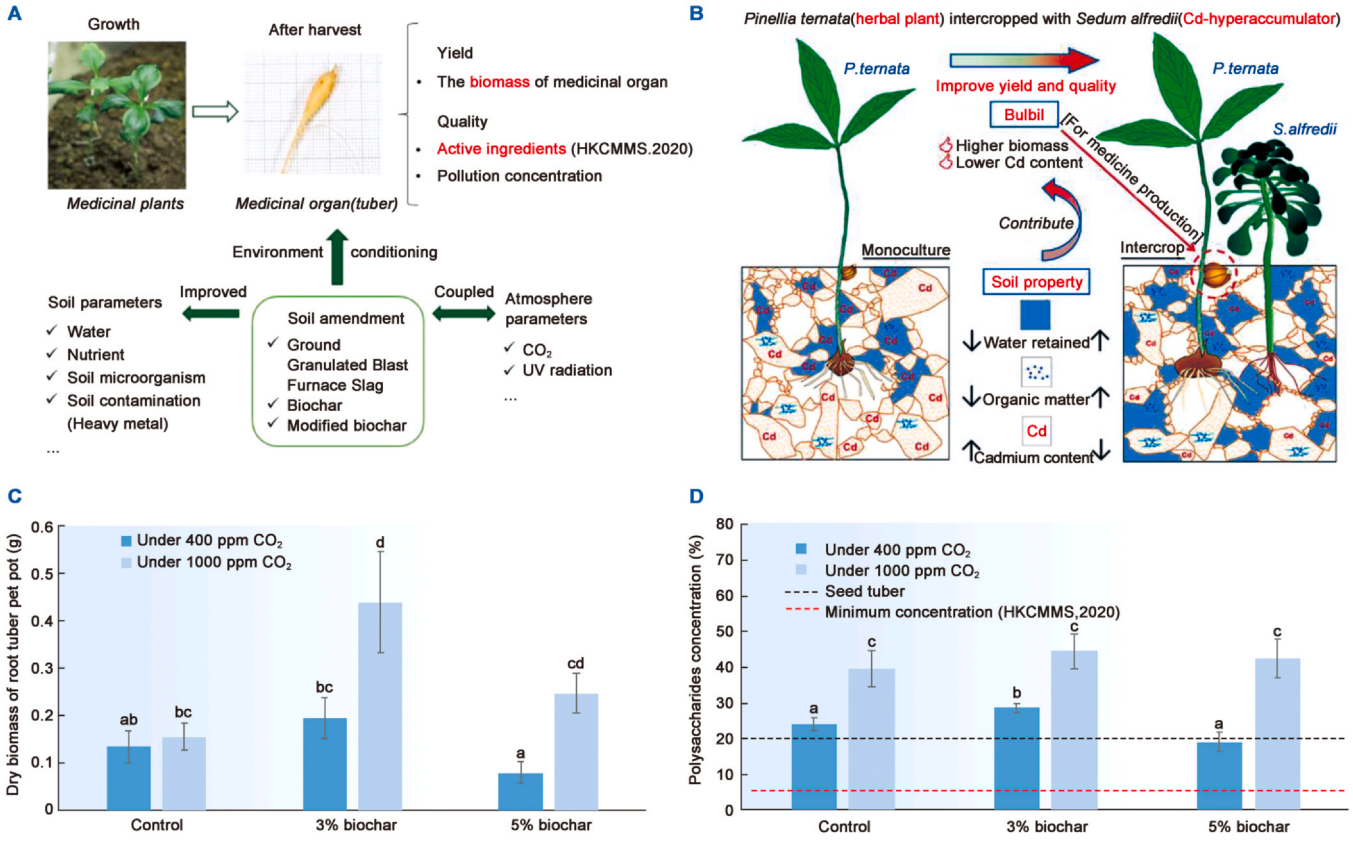

Fig. 5. (**A**) Conceptual framework of factors affecting the yield and quality of medicinal plants; (**B**) Effects of *Pinellia ternata* intercropped with Cd-hyperaccumulator *Sedum alfredii* on the herbal plant–soil system (Ng et al., 2023); Variations in (**C**) biomass and (**D**) polysaccharide concentration of *P. heterophylla* root tuber under different treatments (Ng et al., 2022b).

medicinal plants is hindered by the contamination and poor conditions of soils (Ng et al., 2020c), which can inhibit the production and reduce the quality of medicinal plants. Therefore, efficient agricultural practices should be implemented to enhance the production and quality of medicinal plants. The uptake of water and nutrients by plants is essential for their growth and development (Karthika et al., 2018). This process is governed by Darcy's law (Ni et al., 2017). It indicates that hydraulic gradient, which is proportional to the difference of hydraulic heads between the plant roots and soil, along with the hydraulic conductivity of plant roots play a crucial role in plant water/nutrient uptake (Ng et al., 2022a). Further research is deserved to explore how eco-geotechnics theory can be applied to enhance plant water and nutrient uptake, thereby improving overall plant production.

Biochar represents a cost-effective and environment-friendly soil amendment to improve soil quality and promote plant growth. Ng et al. (2022b) modified peanut shell biochar to improve its characteristics, such as P content and soil water retention, for growing *Pseudostellaria heterophylla*. Their study revealed that compared with unmodified biochar, the modified biochar treatment increased the osmotic suction head and thus the total suction head in the root zone soil due to the enhanced adsorption capability of the ions in the modified biochar (e.g., Na^+). This alleviated the inhibition of root water uptake under high-total-suction conditions, especially when the biochar was applied at a high dosage (e.g., 5 % by mass), thereby facilitating medicinal plant growth. Specifically, the modified biochar enhanced the production of *P. heterophylla* by up to 136 % while increasing the concentration of active ingredients such as polysaccharides and saponins in the medicinal organ by 3 %–79 %. These findings suggest that modified biochar could be an effective soil amendment to enhance the growth and quality of medicinal plants, such as *P. heterophylla*.

Ng et al. (2020c) studied the effects of applying ground granulated blast-furnace slag (GGBS) to *Pinellia ternata* in Cd-contaminated soil. They found that GGBS reduced the concentrations of heavy metals Cd and Cu in plant organs by up to 86 % and 30 %, respectively. At a dosage of 5 % by mass, the application of GGBS increased the production of the root tuber by 46 % while reducing the concentration of active ingredients by up to 36 %. Overall, these findings suggest that GGBS is an effective soil amendment for enhancing the growth of medicinal plants in heavy metal–contaminated soil. In addition to the application of GGBS, Bian et al. (2024) investigated the effects of enzyme-induced carbonate precipitation (EICP) on the remediation of heavy metal-contaminated soil. They concluded that the soluble heavy metals in soil can be transformed into heavy metal carbonates, and the concentrations of Zn^{2+}, Ni^{2+} and Cr(VI) in soil decreased by 99 %, 86 % and 75 %, respectively. Ng et al. (2023) intercropped the medicinal plant *P. ternata* with *Sedum alfredii*, a Cd-hyperaccumulator (Fig. 5B). Based on their findings, the intercropping induced greater water retention due to increased soil pore occupancy by the plant roots, and it also increased the production of organic compounds from root exudates. The yield of the intercropped *P. ternata* was enhanced, which was attributed to the reduction in soil Cd content due to the Cd uptake by *S. alfredii*, as well as improved soil water retention. Thus, intercropping with *S. alfredii* is a feasible method to improve the yield of herbal plants in heavy metal–contaminated soil.

4.3.2. Coupling effects of atmospheric condition and soil conditioner on medicinal plant growth

Atmospheric factors, such as CO_2 concentration and ultraviolet (UV) radiation, play an important role in governing plant growth and metabolism. Recent studies have investigated the combined effects of these atmospheric factors and soil conditioners on medicinal plants. Ng et al. (2022c) investigated how the interaction of CO_2 enrichment with biochar amendments influences the yield and quality of P. heterophylla (Fig. 5C and 5D). In recent years, the ambient atmospheric CO_2 concentration has been approximately 400 ppm. By the end of the 21st century, it is predicted that global atmospheric CO_2 levels could reach up to 1000 ppm, which is the elevated CO_2 concentration used in this study (Ng et al., 2022c). The study revealed that elevated CO_2 levels not only enhanced the mobilisation of the nutrients supplied by the biochar but also increased the RLD, thereby improving the plant's nutrient uptake ability. The results shown in Fig. 5C and D indicate that elevated CO_2 levels (1000 ppm) coupled with 3 % (by mass) biochar could increase the tuber production of *P. heterophylla* by 228 %. Moreover, the concentration of polysaccharides in the medicinal organ was improved by up to 124 % under CO_2 enrichment, enhancing the quality of *P. heterophylla*.

Apart from atmospheric CO_2 concentration, solar UV radiation, including UVA and UVB, has been observed to interact with biochar to influence the growth and quality of *P. heterophylla* (Wang et al., 2023). Specifically, UVA can enhance the production of *P. heterophylla* when biochar is absent. However, when biochar is applied, UV radiation (both UVA and UVB) has no significant effect on the root tuber production of *P. heterophylla*. This suggests that UV radiation and biochar treatment interact negatively in the context of *P. heterophylla* production. Additionally, UVA can significantly improve the generation of polysaccharides when biochar is absent. UV radiation (particularly UVB) also increases the saponin concentration in *P. heterophylla* by up to 79 %, while coupled UVB radiation and biochar treatment significantly improve saponin generation.

5. Research gaps and future research directions

The scientific use of vegetation in the geotechnical field is still in its infancy. Based on the foregoing review and discussion, the following research gaps are identified, along with suggestions on future research directions.

(a) Interactions between vegetation and extreme weather under climate change
The recent increase in the frequency of heat waves (Marx et al., 2021) and droughts (Xu et al., 2019) has exacerbated tree mortality and forest fires, resulting in the decaying of root systems. Such decay can create preferential flow paths that facilitate water infiltration and increase the probability of shallow slope failures. However, the quantitative relationships among root architecture, preferential flow paths, and slope failure patterns remain unclear. Studies on the influence of the architecture of actively growing roots on soil suction response and slope stability have not been comprehensive. Hence, more attention should be paid to the impact of decaying root systems on the ultimate performance of vegetated slopes. Moreover, the increasing frequency of typhoons and rainstorms, especially in Southern China, has been causing more failures of shallow vegetated slopes. Different plant communities (trees, shrubs, grasses, and bamboo) are widely distributed within these regions. Thus, the coupling effects of strong wind and heavy rainfall on the mechanisms of shallow slope failure must be investigated, especially in areas where different plant communities with decayed roots exist.

(b) Soil desiccation cracking and its mitigation in vegetated soils
Soil cracking is commonly observed in dried fine-grained soils. The characterisation of cracking propagation is vital for enhancing the hydro-mechanical performance of earthen infrastructures as cracking can significantly affect water infiltration and soil shear strength. The interactions between vegetation and crack initiation are complex. Some studies have reported that soil cracking can be suppressed through the increase in soil tensile strength provided by root systems (Tang et al., 2012; Song et al., 2017). However, plant roots can also aggravate cracking by restricting the self-healing phenomena in soil and can even proliferate within soil cracks (Sinnathamby et al., 2014; Ghestem et al., 2011). These contrasting observations are highly dependent on the vegetation species, planting strategies, and soil types. Cheng et al. (2023) revealed the

influencing mechanism of planting density on both initiation and propagation of desiccation cracks. It provides valuable insights into investigation of complex interactions between cracks and plant roots. However, the correlations between plant characteristics, soil types, and cracking patterns remain unclear. Further studies should investigate these correlations, quantify their impact on the performance of slopes and earthen covers, and explore potential biomaterials for crack mitigation.

(c) Plant growth and ecological restoration in contaminated sites
Mining is a destructive anthropogenic activity for the landscape and ecosystem. Metal mining can result in high metal concentrations and nutrient deficiency in soil, thereby destroying vegetation and compromising the structure and basic functions of ecosystems. Specifically, soil contamination by heavy metals (e.g., Pb, Hg, and Cd) due to mining activities is extremely harmful to the environment and human health. Hence, post-mining soil remediation is critical for mitigating heavy metal contamination. Many remediation technologies have been developed, including soil replacement, soil amendment, and ecological restoration. In-situ ecological restoration using vegetation is the most attractive option as it is sustainable and cost-effective. Some plant species, such as *Robinia pseudoacacia* and *Ulmus pumila*, can bioaccumulate heavy metals such as Cr, Ni, and Zn, while *Ailanthus altissim* is effective for Cd absorption (Shi et al., 2016). The bioaccumulation and translocation of heavy metals from the soil to plants in mining areas are highly dependent on the hydraulic properties of the unsaturated soil as well as the plant species. Post-mining root growth may also affect soil structures (e.g., PSD and aggregation) and, thus, soil hydraulic properties. Hence, the interactions between plant growth, unsaturated water flow, and heavy metal mobility require further research.

(d) Synergistic influence of vegetation and sustainable soil stabilisers on soil preservation
The frequency of extreme weather events, such as droughts, heat waves, and heavy rainfall, has increased in recent years. This can be ascribed to the deterioration of soil properties, exemplified by damage to soil skeletal structure, soil sealing, soil salinisation, soil desertification, and soil erosion. These challenges can be tackled through soil stabilisation treatments, using substances such as traditional inorganic chemical soil stabilisers (cement or lime) and emerging sustainable alternatives (e.g., biopolymers, biochar, and bacteria-based materials). The utilisation of sustainable soil stabilisers has become a recent research focus on eco-geotechnical engineering. Sustainable amendments can not only enhance soil binding and soil strength but also promote plant growth by providing soil nutrients, increasing soil aeration, and improving soil water retention. In future research, the synergistic effects of sustainable soil stabilisers and vegetation on the hydro-mechanical properties of unsaturated soils should be investigated further to elucidate how these substances suppress the deterioration of soil properties over long periods. Moreover, field trials should be conducted to analyse vegetation–stabiliser interactions, especially under adverse climatic conditions, such as severe drought, high temperature, and heavy rainfall.

(e) Smart sensing of atmosphere–plant–soil interaction in the field
Vegetated can be used as a 'live sensor' as its canopy temperature, leaf colour, and shoot height can reflect plant health and soil water conditions (Boldrin et al., 2019). A combination of remote sensing methods, such as drones and satellites, with deep learning–based image analysis could potentially reveal vegetated soil conditions on a large scale. The provision of real-time soil information could improve the efficiency of water and nutrient usage in 'precision agriculture'. In the engineering field, soil water conditions can be used to evaluate the stability of artificial or natural slopes. If machine learning models are trained on drone or satellite data, highly non-linear relationships between the dependent and independent parameters can be established; thus, machine learning models could outperform conventional models. Trained machine learning models could predict time-dependent canopy characteristics (e.g., leaf area index) and evapotranspiration based on meteorological data collected over large regions. Hence, further studies should focus on the development of atmosphere–plant–soil interaction models based on remote sensing techniques and deep learning. Such models will be invaluable for precision agriculture and the prediction of geological disasters in cities under changing climates.

6. Summary

This state-of-the-art paper reviews the recent advances in the new interdisciplinary field of eco-geotechnics, including an eco-unsaturated soil constitutive model, experimental testing of the hydro-mechanical properties of vegetated soils, and the scope for leveraging the current knowledge. By analysing the research conducted thus far, the scientific gaps are highlighted, and potential directions for future research are suggested; these include the following: (i) interactions between vegetation and extreme weather under climate change, (ii) soil desiccation cracking and its mitigation in vegetated soils, (iii) plant growth and ecological restoration in contaminated sites, (iv) the synergistic influence of vegetation and sustainable soil stabilisers on soil preservation, (v) smart sensing of atmosphere–plant–soil interactions in the field. This review provides a comprehensive outline for future research in eco-geotechnics, which could facilitate the development of resilient geotechnical solutions under climate change.

CRediT authorship contribution statement

Charles Wang Wai Ng: Supervision, Project administration, Funding acquisition, Conceptualization. **Qi Zhang:** Writing – original draft, Investigation, Formal analysis. **Haowen Guo:** Writing – original draft, Validation, Investigation, Formal analysis. **Junjun Ni:** Writing – review & editing, Writing – original draft, Supervision, Project administration, Funding acquisition, Conceptualization. **Yuchen Wang:** Writing – original draft, Validation, Investigation, Data curation. **Anthony Kwan Leung:** Supervision, Project administration, Conceptualization. **Chao Zhou:** Supervision, Project administration, Conceptualization.

Declaration of Competing Interest

The authors declare that they have no known competing financial interests or personal relationships that could have appeared to influence the work reported in this paper.

Acknowledgements

The authors are thankful for the Collaborative Research Fund (Grant No. C5033–23GF) and the Areas of Excellence (AoE) Scheme Fund (Grant No. AoE/E-603/18) awarded by the Hong Kong Research Grants Council under the Government of Hong Kong SAR, China. The corresponding author also would like to thank the National Natural Science Foundation of China (Grant Nos. 52308342 and U2340227) and the Fundamental Research Funds for the Central Universities (Grant Nos. RF1028623071 and 2242024k30066).

References

Albalasmeh, A. A., & Ghezzehei, T. A. (2014). Interplay between soil drying and root exudation in rhizosheath development. *Plant and Soil, 374*, 739–751. https://doi.org/10.1007/s11104-013-1910-y

Albright, W. H., Benson, C. H., Gee, G. W., Roesler, A. C., Abichou, T., Apiwantragoon, P., Lyles, B. F., & Rock, S. A. (2004). Field water balance of landfill covers. *Journal of Environmental Quality, 33*, 2317–2332. https://doi.org/10.2134/jeq2004.2317

Aravena, J. E., Berli, M., Ghezzehei, T. A., & Tyler, S. W. (2011). Effects of root-induced compaction on rhizosphere hydraulic properties – X-ray microtomography imaging and numerical simulations. *Environmental Science Technology, 45*(2), 425–431. https://doi.org/10.1021/es102566j

Bast, A., Wilcke, W., Graf, F., Lüscher, P., & Gärtner, H. (2014). The use of mycorrhiza for eco-engineering measures in steep alpine environments: Effects on soil aggregate formation and fine-root development. *Earth Surface Processes and Landforms, 39*(13), 1753–1763. https://doi.org/10.1002/esp.3557

Been, K., & Jefferies, M. G. (1985). A state parameter for sands. *Géotechnique, 35*(2), 99–112. https://doi.org/10.1680/geot.1985.35.2.99

Bian, Y., Chen, Y. B., Zhan, L. T., Guo, H. W., Ke, H., Wang, Y. Z., Wang, Q. Y., Gao, Y. F., & Gao, Y. Q. (2024). Effects of enzyme-induced carbonate precipitation technique on multiple heavy metals immobilization and unconfined compressive strength improvement of contaminated sand. *Science of The Total Environment, 947*, Article 174409. https://doi.org/10.1016/j.scitotenv.2024.174409

Boldrin, D., Leung, A. K., & Bengough, A. G. (2018). Hydrologic reinforcement induced by contrasting woody species during summer and winter. *Plant and Soil, 427*, 369–390. https://doi.org/10.1007/s11104-018-3640-7

Boldrin, D., Leung, A. K., Bengough, A. G., & Jones, H. G. (2019). Potential of thermal imaging in soil bioengineering to assess plant ability for soil water removal and air cooling. *Ecological Engineering, 141*, Article 105599. https://doi.org/10.1016/j.ecoleng.2019.105599

Boldrin, D., Bengough, A. G., Lin, Z., & Loades, K. W. (2021). Root age influences failure location in grass species during mechanical testing. *Plant and Soil, 461*, 457–469. https://doi.org/10.1007/s11104-020-04824-6

Boldrin, D., Leung, A. K., & Bengough, A. G. (2021). Hydro-mechanical reinforcement of contrasting woody species: A full-scale investigation of a field slope. *Géotechnique, 71*(11), 970–984. https://doi.org/10.1680/jgeot.19.SiP.018

Bordoni, M., Vivaldi, V., Giarola, A., Valentino, R., Bittelli, M., & Meisina, C. (2024). Comparison between mechanical and hydrological reinforcement effects of cultivated plants on shallow slope stability. *Science of the Total Environment, 912*, 168999.

Cai, X. L., Lou, Z. Y., Shimaoka, T., Nakayama, H., Ying, Z., Xiaoyan, C., Komiya, T., Ishizaki, T., & Zhao, Y. Z. (2010). Characteristics of environmental factors and their effects on CH_4 and CO_2 emissions from a closed landfill: An ecological case study of Shanghai. *Waste Management, 30*(3), 446–451. https://doi.org/10.1016/j.wasman.2009.09.047

Chen, G., Weil, R. R., & Hill, R. L. (2014). Effects of compaction and cover crops on soil least limiting water range and air permeability. *Soil and Tillage Research, 136*, 61–69. https://doi.org/10.1016/j.still.2013.09.004

Cheng, Q., Gu, Y. D., Tang, C. S., Zhang, X. Y., & Shi, B. (2023). Desiccation cracking behaviour of a vegetated soil incorporating planting density. *Canadian Geotechnical Journal, 61*(1), 165–173.

Chiu, C. F., & Ng, C. W. W. (2003). A state-dependent elasto-plastic model for saturated and unsaturated soils. *Géotechnique, 53*(9), 809–829. https://doi.org/10.1680/geot.2003.53.9.809

Clarke, J. M., & Townley-Smith, T. F. (1986). Heritability and relationship to yield of excised-leaf water retention in durum wheat. *Crop Science, 26*(2), 289–292. https://doi.org/10.2135/cropsci1986.0011183X002600020016x

Dafalias, Y. F. (1986). Bounding surface plasticity. I: Mathematical foundation and hypoplasticity. *Journal of Engineering Mechanics, 112*(9), 966–987. https://doi.org/10.1061/(ASCE)0733-9399(1986)112:9(966)

Duan, X., Zeng, L., & Sun, X. (2019). Generalized stress framework for unsaturated soil: demonstration and discussion. *Acta Geotechnica, 14*, 1459–1481. https://doi.org/10.1007/s11440-018-0739-1

Ehrmann, J., & Ritz, K. (2014). Plant: soil interactions in temperate multi-cropping production systems. *Plant and Soil, 376*, 1–29. https://doi.org/10.1007/s11104-013-1921-8

Feddes, R. A., Kowalik, P. J., & Zaradny, H. (1978). *Simulation of field water use and crop yield.* New York: John Wiley & Sons.

Feng, S., Liu, H. W., & Ng, C. W. W. (2020). Analytical analysis of the mechanical and hydrological effects of vegetation on shallow slope stability. *Computers and Geotechnics, 118*, Article 103335. https://doi.org/10.1016/j.compgeo.2019.103335

Feng, S., Liu, H. W., & Ng, C. W. W. (2019). Analytical solutions for one-dimensional water flow in vegetated layered soil. *International Journal of Geomechanics, 19*, Article 04018191. https://doi.org/10.1061/(ASCE)GM.1943-5622.0001343

Foresta, V., Capobianco, V., & Cascini, L. (2020). Influence of grass roots on shear strength of pyroclastic soils. *Canadian Geotechnical Journal, 57*(9), 1320–1334. https://doi.org/10.1139/cgj-2019-0142

Gabr, M. A., Akran, M., & Taylor, H. M. (1995). Effect of simulated roots on the permeability of silty soil. *Geotechnical Testing Journal, 18*(1), 112–115. https://doi.org/10.1520/GTJ10127J

Gallipoli, D., Gens, A., Sharma, R., & Vaunat, J. (2003a). An elasto-plastic model for unsaturated soil incorporating the effects of suction and degree of saturation on mechanical behaviour. *Géotechnique, 53*(1), 123–135. https://doi.org/10.1680/geot.2003.53.1.123

Gallipoli, D., Wheeler, S. J., & Karstunen, M. (2003b). Modelling the variation of degree of saturation in a deformable unsaturated soil. *Géotechnique, 53*(1), 105–112. https://doi.org/10.1680/geot.2003.53.1.105

Gens, A., Sánchez, M., & Sheng, D. (2006). On constitutive modelling of unsaturated soils. *Acta Geotechnica, 1*, 137–147. https://doi.org/10.1007/s11440-006-0013-9

Ghestem, M., Sidle, R. C., & Stokes, A. J. B. (2011). The influence of plant root systems on subsurface flow: implications for slope stability. *Bioscience, 61*, 869–879. https://doi.org/10.1525/bio.2011.61.11.6

Ghestem, M., Veylon, G., Bernard, A., Vanel, Q., & Stokes, A. (2014). Influence of plant root system morphology and architectural traits on soil shear resistance. *Plant and Soil, 377*, 43–61. https://doi.org/10.1525/bio.2011.61.11.6

GIA (2022). Herbal medicines - Global market trajectory & analytics. Global Industry Analysts, Inc., California.

Gish, T. J., & Jury, W. A. (1983). Effect of plant roots and root channels on solute transport. *Transactions of the American Society of Agricultural and Biological Engineers, 26*(2), 440–444. https://doi.org/10.13031/2013.33955

Hao, H., Di, H., Jiao, X., Wang, J., Guo, Z., & Shi, Z. (2020). Fine roots benefit soil physical properties key to mitigate soil detachment capacity following the restoration of eroded land. *Plant and Soil, 446*(1), 487–501. https://doi.org/10.1007/s11104-019-04353-x

Huat, B. B. K., Ali, F. H. J., & Low, T. H. (2006). Water infiltration characteristics of unsaturated soil slope and its effect on suction and stability. *Geotechnical and Geological Engineering, 24*(5), 1293–1306. https://doi.org/10.1007/s10706-005-1881-8

Jotisankasa, A., & Sirirattanachat, T. (2017). Effects of grass roots on soil-water retention curve and permeability function. *Canadian Geotechnical Journal, 54*(11), 1612–1622. https://doi.org/10.1139/cgj-2016-0281

Kamchoom, V., Boldrin, D., Leung, A. K., Sookkrajang, C., & Likitlersuang, S. (2022). Biomechanical properties of the growing and decaying roots of *Cynodon dactylon*. *Plant and Soil, 471*, 193–210. https://doi.org/10.1007/s11104-021-05207-1

Karr, L., Harre, B. & Hakonson, T.E. (1999). Infiltration control landfill cover demonstration at Marine Corps Base, Hawaii. Technical Report TR-2108-ENV, Naval Facilities Engineering Service Center, Port Hueneme, CA.

Karthika, K. S., Rashmi, I., & Parvathi, M. S. (2018). Biological functions, uptake and transport of essential nutrients in relation to plant growth. *Plant Nutrients and Abiotic Stress Tolerance,* 1–49. https://doi.org/10.1007/978-981-10-9044-8_1

Kim, J. H., Fourcaud, T., Jourdan, C., Maeght, J. L., Mao, Z., Metayer, J., & Stokes, A. (2017). Vegetation as a driver of temporal variations in slope stability: The impact of hydrological processes. *Geophysical Research Letters, 44*(10), 4897–4907. https://doi.org/10.1002/2017GL073174

Leung, A. K., Kamchoom, V., & Ng, C. W. W. (2017). Influences of root-induced soil suction and root geometry on slope stability: A centrifuge study. *Canadian Geotechnical Journal, 54*(3), 291–303. https://doi.org/10.1139/cgj-2015-0263

Leung, A. K., Garg, A., & Ng, C. W. W. (2015a). Effects of plant roots on soil-water retention and induced suction in vegetated soil. *Engineering Geology, 193*, 183–197. https://doi.org/10.1016/j.enggeo.2015.04.017

Leung, A. K., Garg, A., Coo, J. L., Ng, C. W. W., & Hau, B. C. H. (2015b). Effects of the roots of *Cynodon dactylon* and *Shefflera heptaphylla* on water infiltration rate and soil hydraulic conductivity. *Hydrological Processes, 29*(15), 3342–3354. https://doi.org/10.1002/hyp.10452

Lee, J. T., Shih, C. Y., & Hsu, Y. S. (2023). Root biomechanical features and wind erosion resistance of three native leguminous psammophytes for coastal dune restoration. *Ecological Engineering, 191*, Article 106966. https://doi.org/10.1016/j.ecoleng.2023.106966

Li, C., Cheng, Q., Tang, C., Gu, Y., Cui, L., & Guo, H. (2024). Effects of layer thickness on desiccation cracking behaviour of a vegetated soil. *Biogeotechnics, 2*(2), Article 100068. https://doi.org/10.1016/j.bgtech.2023.100068

Li, X. S. (2005). Modelling of hysteresis response for arbitrary wetting/drying paths. *Computers and Geotechnics, 32*(2), 133–137. https://doi.org/10.1016/j.compgeo.2004.12.002

Li, Y., & Ghodrati, M. (1994). Preferential transport of nitrate through soil columns containing root channels. *Soil Science Society of America Journal, 58*, 653–659. https://doi.org/10.2136/sssaj1994.03615995005800030003x

Liang, T., Knappett, J. A., Bengough, A. G., & Ke, Y. X. (2017). Small-scale modelling of plant root systems using 3D printing, with applications to investigate the role of vegetation on earthquake-induced landslides. *Landslides, 14*, 1747–1765. https://doi.org/10.1007/s10346-017-0802-2

Liu, H. W., Feng, S., Garg, A., & Ng, C. W. W. (2018). Analytical solutions of pore-water pressure distributions in a vegetated multi-layered slope considering the effects of roots on water permeability. *Computers and Geotechnics, 102*, 252–261. https://doi.org/10.1016/j.compgeo.2018.06.003

Löbmann, M. T., Geitner, C., Wellstein, C., & Zerbe, S. (2020). The influence of herbaceous vegetation on slope stability–A review. *Earth-Science Reviews, 209*, Article 103328. https://doi.org/10.1016/j.earscirev.2020.103328

Lu, J., Zhang, Q., Werner, A. D., Li, Y., Jiang, S., & Tan, Z. (2020). Root-induced changes of soil hydraulic properties–A review. *Journal of Hydrology, 589*, Article 125203. https://doi.org/10.1007/s11104-014-2121-x

Marx, W., Haunschild, R., & Bornmann, L. (2021). Heat waves: A hot topic in climate change research. *Theoretical and Applied Climatology, 146*(1), 781–800. https://doi.org/10.1007/s00704-021-03758-y

Melchior, S. (1997). In-situ studies of the performance of landfill caps (compacted soil liners, geomembranes, geosynthetic clay liners and capillary barriers). *Land Contamination Reclamation, 5*(3), 209–216.

Ng, C.W.W., Kamchoom, V., Leung, A.K., et al. (2016c). A novel system for simulating water transportation in porous medium (in Chinese). China Patent, CN103424345B.

Ng, C. W. W., Kamchoom, V., & Leung, A. K. (2016d). Centrifuge modelling of the effects of root geometry on transpiration-induced suction and stability of vegetated slopes. *Landslides, 13*, 925–938. https://doi.org/10.1007/s10346-015-0645-7

Ng, C. W. W., Leung, A. K., Kamchoom, V., & Garg, A. (2014b). A novel root system for simulating transpiration-induced soil suction in centrifuge. *Geotechnical Testing Journal, 37*(5), 733–747. https://doi.org/10.1520/GTJ20130116

Ng, C. W. W., Liu, H. W., & Feng, S. (2015a). Analytical solutions for calculating pore-water pressure in an infinite unsaturated slope with different root architectures. *Canadian Geotechnical Journal, 52*(12), 1981–1992. https://doi.org/10.1139/cgj-2015-0001

Ng, C.W.W., Xu, J. & Chen, R. (2015b). All-weather landfill soil cover system for preventing water infiltration and landfill gas emission. US Patent, US9101968B2.

Ng, C. W. W. (2017). Atmosphere-plant-soil interactions: theories and mechanisms (in Chinese). *Chinese Journal of Geotechnical Journal, 39*, 1–47. https://doi.org/10.11779/CJGE201701001

Ng, C. W. W. (2014). The state-of-the-art centrifuge modelling of geotechnical problems at HKUST. *Journal of Zhejiang University Science A, 15*(1), 1–21. https://doi.org/10.1631/jzus.A1300217

Ng, C. W. W., & Leung, A. K. (2012). Measurements of drying and wetting permeability functions using a new stress-controllable soil column. *Journal Geotechnical and Geoenvironmental Engineering, 138*(1), 58–68. https://doi.org/10.1061/(ASCE)GT.1943-5606.0000560

Ng, C. W. W., & Pang, Y. W. (2000). Experimental investigations of the soil-water characteristics of a volcanic soil. *Canadian Geotechnical Journal, 37*(6), 1252–1264. https://doi.org/10.1139/t00-056

Ng, C. W. W., & Yung, S. Y. (2008). Determination of the anisotropic shear stiffness of an unsaturated decomposed soil. *Géotechnique, 58*(1), 23–35. https://doi.org/10.1680/geot.2008.58.1.23

Ng, C. W. W., Leung, A. K., & Woon, K. X. (2014a). Effect of soil density on grass-induced suction distributions in compacted soil subjected to rainfall. *Canadian Geotechnical Journal, 51*(3), 311–321. https://doi.org/10.1139/cgj-2013-0221

Ng, C. W. W., Ni, J. J., Leung, A. K., & Wang, Z. J. (2016a). A new and simple water retention model for root-permeated soils. *Géotechnique Letters, 6*(1), 106–111. https://doi.org/10.1680/jgele.15.00187

Ng, C. W. W., Ni, J. J., Leung, A. K., Zhou, C., & Wang, Z. J. (2016b). Effects of planting density on tree growth and induced soil suction. *Géotechnique, 66*(9), 711–724. https://doi.org/10.1680/jgeot.15.P.196

Ng, C. W. W., Ni, J. J., & Leung, A. K. (2020b). Effects of plant growth and spacing on soil hydrological changes: A field study. *Géotechnique, 70*(10), 867–881. https://doi.org/10.1680/jgeot.18.P.207

Ng, C. W. W., Zhang, Q., Zhang, S., Lau, S. Y., Guo, H., & Li, Z. (2024a). A new state-dependent constitutive model for cyclic thermo-mechanical behaviour of unsaturated vegetated soil. *Canadian Geotechnical Journal, 61*(10), 2155–2179. https://doi.org/10.1139/cgj-2023-0268

Ng, C. W. W., Zhou, C., & Chiu, C. F. (2020a). Constitutive modelling of state-dependent behaviour of unsaturated soils: An overview. *Acta Geotechnica, 15*(10), 2705–2725. https://doi.org/10.1007/s11440-020-01014-7

Ng, C. W. W., Chen, R., Coo, J., Liu, J., Ni, J. J., Chen, Y. M., Zhan, L. T., Guo, H. W., & Lu, B. W. (2019). A novel vegetated three-layer landfill cover system using recycled construction wastes without geomembrane. *Canadian Geotechnical Journal, 56*(12), 1863–1875. https://doi.org/10.1139/cgj-2017-0728

Ng, C. W. W., Chowdhury, N., & Wong, J. T. F. (2020c). Effects of ground granulated blast-furnace slag (GGBS) on hydrological responses of Cd-contaminated soil planted with a herbal medicinal plant (*Pinellia ternata*). *Canadian Geotechnical Journal, 57*(5), 673–682. https://doi.org/10.1139/cgj-2018-0868

Ng, C. W. W., Guo, H. W., Ni, J. J., Chen, R., Xue, Q., Zhang, Y. M., Feng, Y., Chen, Z. K., Feng, S., & Zhang, Q. (2024b). Long-term field performance of non-vegetated and vegetated three-layer landfill cover systems using construction waste without geomembrane. *Géotechnique, 74*(2), 155–173. https://doi.org/10.1680/jgeot.21.00238

Ng, C. W. W., San So, P., Wong, J. T. F., & Lau, S. Y. (2023). Intercropping of *Pinellia ternata* (herbal plant) with *Sedum alfredii* (Cd-hyperaccumulator) to reduce soil cadmium (Cd) absorption and improve yield. *Environmental Pollution, 318*, Article 120930. https://doi.org/10.1016/j.envpol.2022.120930

Ng, C. W. W., Zhang, Q., Ni, J., & Li, Z. (2021). A new three-dimensional theoretical model for analysing the stability of vegetated slopes with different root architectures and planting patterns. *Computers and Geotechnics, 130*, Article 103912. https://doi.org/10.1016/j.compgeo.2020.103912

Ng, C. W. W., Zhang, Q., Zhou, C., & Ni, J. J. (2022a). Eco-geotechnics for human sustainability. *Science China Technological Sciences, 65*(12), 2809–2845. https://doi.org/10.1007/s11431-022-2174-9

Ng, C. W. W., Wang, Y. C., Ni, J. J., & So, P. S. (2022b). Effects of phosphorus-modified biochar as a soil amendment on the growth and quality of *Pseudostellaria heterophylla*. *Scientific Reports, 12*(1), 7268. https://doi.org/10.1038/s41598-022-11170-3

Ng, C. W. W., Wang, Y. C., Ni, J. J., & Tsim, K. W. K. (2022c). Coupled effects of CO_2 and biochar amendment on the yield and quality of *Pseudostellaria heterophylla*. *Industrial Crops and Products, 188*, Article 115599. https://doi.org/10.1016/j.indcrop.2022.115599

Ni, J. J., Leung, A. K., & Ng, C. W. W. (2017). Investigation of plant growth and transpiration-induced matric suction under mixed grass-tree conditions. *Canadian Geotechnical Journal, 54*(4), 561–573. https://doi.org/10.1139/cgj-2016-0226

Ni, J. J., Leung, A. K., Ng, C. W. W., & Shao, W. (2018a). Modelling hydro-mechanical reinforcements of plants to slope stability. *Computers and Geotechnics, 95*, 99–109. https://doi.org/10.1016/j.compgeo.2017.09.001

Ni, J. J., Leung, A. K., & Ng, C. W. W. (2018b). Modelling soil suction changes due to mixed species planting. *Ecological Engineering, 117*, 1–17. https://doi.org/10.1016/j.ecoleng.2018.02.023

Ni, J. J., Leung, A. K., & Ng, C. W. W. (2019a). Modelling effects of root growth and decay on soil water retention and permeability. *Canadian Geotechnical Journal, 56*(7), 1049–1055. https://doi.org/10.1139/cgj-2018-0402

Ni, J. J., Leung, A. K., & Ng, C. W. W. (2019b). Influences of plant spacing on root tensile strength of *Schefflera arboricola* and soil shear strength. *Landscape and Ecological Engineering, 15*(2), 223–230. https://doi.org/10.1007/s11355-019-00374-x

Ni, J. J., & Ng, C. W. W. (2019). Long-term effects of grass roots on gas permeability in unsaturated simulated landfill covers. *Science of the Total Environment, 666*, 680–684. https://doi.org/10.1016/j.scitotenv.2019.02.248

Ni, J. J., Liu, S. S., Huang, Y., & Gao, Y. F. (2024). Temperature and plant root effects on soil hydrological response and slope stability. *Computers and Geotechnics, 174*, Article 106663. https://doi.org/10.1016/j.compgeo.2024.106663

Ni, J. J., Zhou, J., Wang, Y., & Guo, H. (2023). Gas permeability and emission in unsaturated vegetated landfill cover with biochar addition. *Biochar, 5*(1), 47. https://doi.org/10.1007/s42773-023-00246-6

Nyhan, J. W., Hakonson, T. E., & Drennon, B. J. (1990). A water balance study of two landfill cover designs for semiarid regions. *Journal of Environmental Quality, 19*, 281–288. https://doi.org/10.2134/jeq1990.00472425001900020014x

Pallewattha, M., Indraratna, B., Heitor, A., & Rujikiatkamjorn, C. (2019). Shear strength of a vegetated soil incorporating both root reinforcement and suction. *Transportation Geotechnics, 18*, 72–82. https://doi.org/10.1016/j.trgeo.2018.11.005

Prasad, R. (1988). A linear root water uptake model. *Journal of Hydrology, 99*, 297–306. https://doi.org/10.1016/0022-1694(88)90055-8

Phillips, C. J., & Watson, A. J. (1994). *Structural tree root research in New Zealand: A review. Landcare research science series.* Manaaki Whenua Press71 (No7).

Pollen-Bankhead, N., & Simon, A. (2010). Hydrologic and hydraulic effects of riparian root networks on streambank stability: Is mechanical root-reinforcement the whole story? *Geomorphology, 116*(3-4), 353–362. https://doi.org/10.1016/j.geomorph.2009.11.013

Raats, P. A. C. (1974). Steady flows of water and salt in uniform soil profiles with plant roots. *Soil Science Society of America Journal, 38*, 717–722. https://doi.org/10.2136/sssaj1974.03615995003800050012x

Rahardjo, H., Satyanaga, A., Leong, E. C., Santoso, V. A., & Ng, Y. S. (2014). Performance of an instrumented slope covered with shrubs and deep-rooted grass. *Soils and Foundations, 54*(3), 417–425. https://doi.org/10.1016/j.sandf.2014.04.010

Romero, E., Gens, A., & Lloret, A. (1999). Water permeability, water retention and microstructure of unsaturated compacted boom clay. *Engineering Geology, 54*(1-2), 117–127. https://doi.org/10.1016/S0013-7952(99)00067-8

Russell, A. R., & Khalili, N. (2006). A unified bounding surface plasticity model for unsaturated soils. *International Journal for Numerical and Analytical Methods in Geomechanics, 30*(3), 181–212. https://doi.org/10.1002/nag.475

Scanlan, C.A. (2009). Processes and effects of root-induced changes to soil hydraulic properties. PhD Thesis, University of Western Australia, Australia.

Scanlan, C.A., & Hinz, C. (2010). Insight into the processes and effects of root induced changes to soil hydraulic properties. In: Proceedings of the 19th World Congress of Soil Science, Soil Solutions for a Changing World, Brisbane, Australia, vol. 2, pp. 41-44.

Scholl, P., Leitner, D., Kammerer, G., Lioskandl, W., Kaul, H. P., & Bodner, G. (2014). Root induced changes of effective 1D hydraulic properties in a soil column. *Plant and Soil, 381*(1-2), 193–213. https://doi.org/10.1007/s11104-014-2121-x

Shao, W., Ni, J. J., Leung, A. K., Su, Y., & Ng, C. W. W. (2017). Analysis of plant root-induced preferential flow and pore-water pressure variation by a dual-permeability model. *Canadian Geotechnical Journal, 54*(11), 1537–1552. https://doi.org/10.1139/cgj-2016-0629

Sheng, D., Fredlund, D. G., & Gens, A. (2008). A new modelling approach for unsaturated soils using independent stress variables. *Canadian Geotechnical Journal, 45*(4), 511–534. https://doi.org/10.1139/T07-112

Shi, Y. K., Mu, X. M., Li, K. R., & Shao, H. B. (2016). Soil characterization and differential patterns of heavy metal accumulation in woody plants grown in coal gangue wastelands in Shaanxi, China. *Environmental Science and Pollution Research, 23*, 13489–13497. https://doi.org/10.1007/s11356-016-6432-8

Shwetha, P., & Varija, K. (2015). Soil water retention curve from saturated hydraulic conductivity for sandy loam and loamy sand textured soils. *Aquatic Procedia, 4*, 1142–1149. https://doi.org/10.1016/j.aqpro.2015.02.145

Sidle, R. C., & Ochiai, H. (2007). Landslides processes, prediction, and land use water resources monograph 18. *Natural resources forum, 31*(4), 322–326.

Sidle, R. C., & Bogaard, T. A. (2016). Dynamic earth system and ecological controls of rainfall-initiated landslides. *Earth Science Reviews, 159*, 275–291. https://doi.org/10.1016/j.earscirev.2016.05.013

Sinnathamby, G., Phillips, D. H., Sivakumar, V., & Paksy, A. (2014). Landfill cap models under simulated climate change precipitation: impacts of cracks and root growth. *Géotechnique, 64*(2), 95–107. https://doi.org/10.1007/s12665-024-11604-3

Somers, B., & Asner, G. P. (2013). Multi-temporal hyperspectral mixture analysis and feature selection for invasive species mapping in rainforests. *Remote Sensing of Environment, 136*, 14–27. https://doi.org/10.1016/j.rse.2013.04.006

Song, L., Li, J. H., Zhou, T., & Fredlund, D. G. (2017). Experimental study on unsaturated hydraulic properties of vegetated soil. *Ecological Engineering, 103*, 207–216. https://doi.org/10.1016/j.ecoleng.2017.04.013

Sonnenberg, R., Bransby, M. F., Hallett, P. D., Bengough, A. G., Mickovski, S. B., & Davies, M. C. R. (2010). Centrifuge modelling of soil slopes reinforced with vegetation. *Canadian Geotechnical Journal, 47*(12), 1415–1430. https://doi.org/10.1139/T10-037

Świtała, B. M., & Wu, W. (2018). Numerical modelling of rainfall-induced instability of vegetated slopes. *Géotechnique, 68*(6), 481–491. https://doi.org/10.1680/jgeot.16.P.176

Tang, A. M., & Cui, Y. J. (2009). Modelling the thermomechanical volume change behaviour of compacted expansive clays. *Géotechnique, 59*(3), 185–195. https://doi.org/10.1680/geot.2009.59.3.185

Tang, C. S., Shi, B., Cui, Y. J., Liu, C., & Gu, K. (2012). Desiccation cracking behavior of polypropylene fiber–reinforced clayey soil. *Canadian Geotechnical Journal, 49*(9), 1088–1101. https://doi.org/10.1139/t2012-067

United States Environmental Protection Agency (USEPA). (1993). Solid waste disposal facility criteria, Technical manual EPA530-R-93-017, Washington, DC.

van Genuchten, M. T. (1980). A closed-form equation for predicting the hydraulic conductivity of unsaturated soils. *Soil Science Society of America Journal, 4*(5), 892–898. https://doi.org/10.2136/sssaj1980.03615995004400050002x

Vardanega, P. J., & Bolton, M. D. (2013). Stiffness of clays and silts: Normalizing shear modulus and shear strain. *Journal of Geotechnical and Geoenvironmental Engineering, 139*(9), 1575–1589. https://doi.org/10.1061/(ASCE)GT.1943-5606.0000887

Vergani, C., & Graf, F. (2016). Soil permeability, aggregate stability and root growth: A pot experiment from a soil bioengineering perspective. *Ecohydrology, 9*(5), 830–842. https://doi.org/10.1002/eco.1686

Wahren, A., Feger, K. H., Schwärzel, K., & Münch, A. (2009). Land-use effects on flood generation–considering soil hydraulic measurements in modelling. *Advances in Geosciences, 21*, 99–107. https://doi.org/10.5194/adgeo-21-99-2009

Wang, X., Hong, M. M., Huang, Z., Zhao, Y. F., Ou, Y. S., Jia, H. X., & Li, J. (2019). Biomechanical properties of plant root systems and their ability to stabilize slopes in geohazard-prone regions. *Soil and Tillage Research, 189*, 148–157. https://doi.org/10.1016/j.still.2019.02.003

Wang, Y. C., Ng, C. W. W., & Ni, J. J. (2023). Interactive effects of ultraviolet irradiation and biochar treatment on the growth and active ingredients of *Pseudostellaria heterophylla*. *Journal of Plant Growth Regulation, 42*, 7660–7672. https://doi.org/10.1007/s00344-023-11041-9

Warren, R. W., Hakonson, T. E., & Bostick, K. V. (1996). Choosing the most effective hazardous waste landfill cover. *Remediation Journal, 6*(2), 23–41. https://doi.org/10.1002/rem.3440060205

Wheeler, S. J., Sharma, R. S., & Buisson, M. S. R. (2003). Coupling of hydraulic hysteresis and stress–strain behaviour in unsaturated soils. *Géotechnique, 53*(1), 41–54. https://doi.org/10.1680/geot.2003.53.1.41

WHO (2013). *WHO traditional medicine strategy: 2014–2023.* Switzerland: World Health Organization.

Woodman, N. D., Smethurst, J. A., Roose, T., Powrie, W., Meijer, G. J., Knappett, J. A., & Dias, T. (2020). Mathematical and computational modelling of vegetated soil incorporating hydraulically-driven finite strain deformation. *Computers and Geotechnics, 127*, Article 103754. https://doi.org/10.1016/j.compgeo.2020.103754

Xiong, Y., Ye, G., Zhu, H., Zhang, S., & Zhang, F. (2016). Thermoelastoplastic constitutive model for unsaturated soils. *Acta Geotechnica, 11*(6), 1287–1302. https://doi.org/10.1007/s11440-016-0462-8

Xu, C., McDowell, N. G., Fisher, R. A., Wei, L., Sevanto, S., Christoffersen, B. O., Weng, E., & Middleton, R. S. (2019). Increasing impacts of extreme droughts on vegetation productivity under climate change. *Nature Climate Change, 9*(12), 948–953. https://doi.org/10.1038/s41558-019-0630-6

Xu, K., Huang, M., Liu, Z., Cui, M., & Li, S. (2023). Mechanical properties and disintegration behavior of EICP-reinforced sea sand subjected to drying-wetting cycles. *Biogeotechnics, 1*(2), Article 100019. https://doi.org/10.1016/j.bgtech.2023.100019

Yan, W. M., & Zhang, G. H. (2015). Soil-water characteristics of compacted sandy and cemented soils with and without vegetation. *Canadian Geotechnical Journal, 52*(9), 1–14. https://doi.org/10.1139/cgj-2014-0334

Zhan, T. L., Jia, G. W., Chen, Y. M., Fredlund, D. G., & Li, H. (2013). An analytical solution for rainfall infiltration into an unsaturated infinite slope and its application to slope stability analysis. *International Journal for Numerical and Analytical Methods in Geomechanics, 37*(12), 1737–1760. https://doi.org/10.1002/nag.2106

Zhang, Q. (2024). Cyclic thermo-hydro-mechanical behaviour of vegetated soil slope under climate change: constitutive and numerical modelling. PhD thesis, The Hong Kong University of Science and Technology, Hong Kong SAR, China.

Zhou, C., & Ng, C. W. W. (2014). A new and simple stress-dependent water retention model for unsaturated soil. *Computers and Geotechnics, 62*, 216–222. https://doi.org/10.1016/j.compgeo.2014.07.012

Lei, M. Y., Cui, Y. F., Ni, J. J., Zhang, G. T., Li, Y., Wang, H., Liu, D. Z., Yi, S. J., Jin, W., & Zhou, L. Q. (2022). Temporal evolution of the hydromechanical properties of soil-root systems in a forest fire in China. *Science of the Total Environment, 809*, Article 151165. https://doi.org/10.1016/j.scitotenv.2021.151165